# SEISMIC STRENGTHENING OF A REINFORCED CONCRETE FRAME USING STRUCTURAL STEEL BRACING

by

Elizabeth A. Jones

and

James O. Jirsa

Report on a Research Project

Sponsored by

National Science Foundation

Grant No. CEE-8201205

Phil M. Ferguson Structural Engineering Laboratory
Department of Civil Engineering
BUREAU OF ENGINEERING RESEARCH
THE UNIVERSITY OF TEXAS AT AUSTIN

May 1986

50272-101

| REPORT DOCUMENTATION PAGE | 1. REPORT NO. | 2. | 3. Recipient's Accession No. |
|---|---|---|---|

**4. Title and Subtitle**

SEISMIC STRENGTHENING OF A REINFORCED CONCRETE FRAME USING STRUCTURAL STEEL BRACING

**5. Report Date** May 1986

**6.**

**7. Author(s)**

Elizabeth A. Jones and James O. Jirsa

**8. Performing Organization Rept. No.** PMFSEL 86-5

**9. Performing Organization Name and Address**

Phil M. Ferguson Structural Engineering Laboratory
The University of Texas at Austin
10100 Burnet Road
Austin, TX 78758

**10. Project/Task/Work Unit No.**

**11. Contract(C) or Grant(G) No.**

(C)

(G) CEE - 8201205

**12. Sponsoring Organization Name and Address**

National Science Foundation
Washington, D.C.

**13. Type of Report & Period Covered**

**14.**

**15. Supplementary Notes**

**16. Abstract (Limit: 200 words)**

A two-thirds scale model of two bays and two stories of the exterior moment resisting frame of a reinforced concrete building was constructed. The test specimen, which had deep spandrel beams and short narrow columns, was strengthened with an exposed structural steel diagonal bracing scheme in order to increase the lateral capacity of the structure for earthquake loads. Construction and fabrication of the strengthening scheme are discussed.

The model was subjected to reversed, cyclic loads producing maximum interstory drifts of 1.3 percent. The behavior of the model is discussed, with special emphasis on the load-drift relationships of the frame. The load carried by the wide flange braces and the forces carried in steel collector members are examined. Slip between the steel elements and the concrete frame was also measured. The importance of quality control in fabrication of epoxy-grouted bolts used to attach the steel collectors to the concrete frame and of welded brace connections is discussed.

**17. Document Analysis a. Descriptors**

Structural Engineering
Earthquake Engineering
Reinforced Concrete
Buildings
Repairs
Strengthening
Steel Braces
Cyclic Loading
Testing
Lateral Forces
Buckling

**b. Identifiers/Open-Ended Terms**

**c. COSATI Field/Group**

**18. Availability Statement**

**19. Security Class (This Report)** Unclassified

**20. Security Class (This Page)**

**21. No. of Pages**

**22. Price**

(See ANSI-Z39.18) See Instructions on Reverse OPTIONAL FORM 272 (4-77) (Formerly NTIS-35) Department of Commerce

TABLE OF CONTENTS

LIST OF TABLES

LIST OF FIGURES (continued)

LIST OF FIGURES (continued)

LIST OF FIGURES (continued)

# CHAPTER 1

# INTRODUCTION

## 1.1 Need for Strengthening

Many existing structures in high risk earthquake areas are inadequate in their ability to withstand seismic loads. Although these buildings were designed and constructed following the structural codes in effect at the time, their lateral-load resisting systems are deficient in terms of the stricter and more complex codes of today.

Significant changes in the Structural Engineers Association of California Recommended Lateral Force Requirements and Commentary [1], have taken place in the past fifteen years. The SEAOC code, which serves as a standard for many regional and city codes, was altered as a result of earthquake engineering research funded after the 1971 San Fernando Earthquake. Major changes in the specifications involved proportioning of members and reinforcement details in reinforced concrete structures.

Often, an owner will choose to strengthen, as well as repair, a building damaged by an earthquake rather than construct a new building. Other reasons for seismic strengthening include forced compliance with local building codes caused by changes in occupancy, and voluntary measures taken by owners for safety or financial interests.

## 1.2 Strengthening Techniques

Some of the more common methods of seismic strengthening are shown in Fig. 1.1. These include infilling walls, adding wingwalls to existing columns, attaching structural steel braces, and encasing columns. In general, the first three methods are regarded as techniques to increase strength. Encasing columns may be used to increase ductility rather than strength.

The purpose of column encasement is to improve the shear strength of the columns, thereby increasing the ductility of the structure by avoiding a brittle shear failure. The "wrapping" techniques include steel straps welded to steel angles at each corner, a steel case filled with grout, or a concrete coat with a steel mesh. When a column is encased, an increase in flexural

capacity which would result in a shear failure mechanism must be avoided. Often a gap is left at the ends of a column to prevent an increase in flexural capacity.

Wingwalls, or side walls, can be precast or cast-in-place elements attached to the existing columns. By increasing both the flexural and shear strength of columns, addition of wingwalls will usually transfer the failure mechanism from the columns to the beams. Anchorage of the vertical steel reinforcement in the wingwalls must be provided in one of two ways. Either the steel is embedded in the beams above and below, or the vertical bars are continued through sections of the wingwalls which are cast against the beam faces. The most important detail in the design of wingwalls is the connection between the new and old concrete. Shear transfer between the old and new may be accomplished through an arrangement of shear keys, or by grouted dowels or wedge anchors into the existing elements.

Several steel bracing arrangements are shown in Fig. 1.2. Possible patterns include X-braces, K-shape, diamond shape, and eccentric braces. Steel bracing can be designed to carry all or part of the lateral design loads. An important consideration is the transfer of load from the concrete frame to the steel system. Vertical and horizontal steel members, which are attached to the concrete columns and beams, may be used to make this transfer.

The selection of a strengthening method depends on the desired result: an increase in strength, an increase in ductility, or a combination of the two. Aesthetics, economics, and construction are all important factors to consider when choosing a strengthening scheme. In order to minimize interference with the normal operation of a building, it is vital to consider the method of construction.

## 1.3 Example

The most likely candidate for seismic strengthening is a building which has satisfactory gravity load capacity, is clearly deficient in its lateral load system, and is economically feasible to strengthen. In the United States, structures meeting the above conditions are a number of reinforced concrete buildings constructed in California during the 1950's and 1960's.

During this time period, the trend was to concentrate the lateral resistance in the exterior frames and leave the interior frames as flat slabs on columns. This type of design

allowed larger vertical clearances on the interior and, thus, a reduction in the overall height of the building. Because the lateral earthquake design loads were much lower thirty years ago, it was possible to carry the loads entirely in the outer frames.

Due to the increase in earthquake design loads, these outer frames are not strong enough by today's standards. In addition, the columns are underdesigned because the building codes at the time did not emphasize the possibility of shear failure in columns, nor did they offer the detailing requirements which are now in use. Therefore, it is economically feasible to strengthen the exterior frames only on these structures and, thus, reduce the interference with the function of the building.

A specific example of the type of building suitable for seismic strengthening is the weak column/strong beam system shown in Fig. 1.3. The exterior moment-resisting frame consists of deep spandrel beams framing into slender columns. The weak link of the example building is the short column, often referred to as a "captive" column. These columns are sometimes created when non-structural walls are added which reduce the clear height of the columns. Figure 1.4 shows the relationship between the moments and shears in a column subjected to lateral load. As the length (L) of a column is decreased, the shear force (V) increases for a given end moment (M) resulting from the displacement ($\Delta$).

The columns of the example building will fail under lateral load long before the beams develop their flexural strength. The column shear failure will be brittle, resulting in a sudden loss of capacity and a possible collapse of the structure. Figure 1.5 shows the brittle column failure of a high school building in Japan, which took place during the 1968 Tokachi-Oki Earthquake. The failure occurred in the captive region of the column between the infilled walls.

To strengthen the weak column/strong beam building, it is necessary to increase the shear capacity of the columns or to carry the shear by an alternate load resisting system in order to change the failure mechanism of the structure. To achieve an increase in shear capacity, the columns could be strengthened by encasement. Alternatively, wingwalls could be added which would raise both the flexural and shear capacity. Another option would be to install steel bracing on the exterior frames. If the braces are designed to carry the entire lateral load, column shear failure can be avoided.

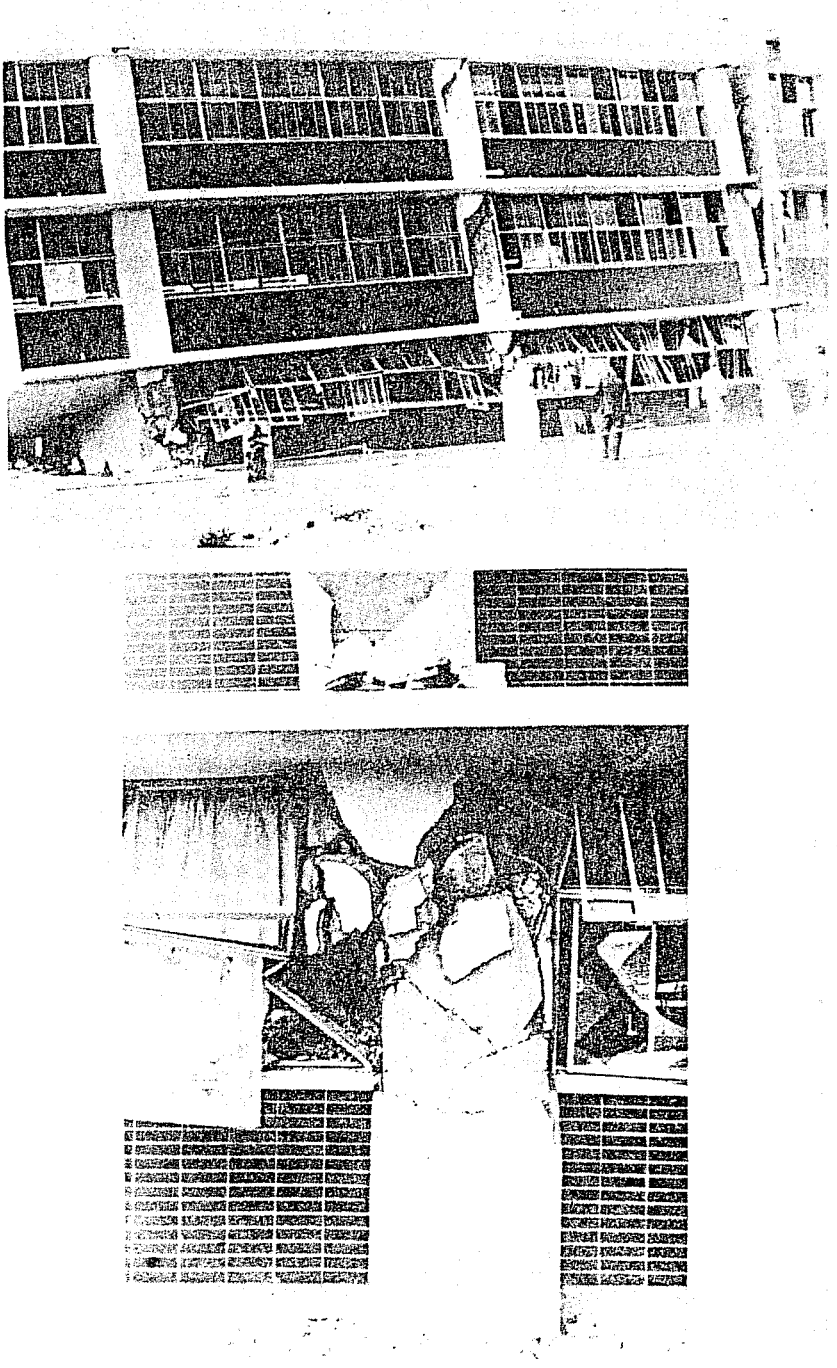

Fig. 1.5 Column Failure in Japanese Building - 1968 Tokachi-Oki Earthquake [4]

Oki Earthquake. Most of the damage was caused by shear failure of columns in low to middle rise buildings [5]. Many structures were strengthened even though there were no guidelines at the time.

In 1977, an advisory committee to the Japanese Ministry of Construction prepared design guidelines which were published by the Japan Building Disaster Prevention Association. The "Guideline for Seismic Retrofitting (Strengthening, Toughening, and/or Stiffening) Design of Existing Reinforced Concrete Buildings" [6,7] was meant to be used in conjunction with a guideline for evaluation of existing buildings for their seismic safety. The 1977 design guideline provided calculation procedures for infilled walls, wingwalls, and reinforced columnns.

After the Miyagiken-Oki Earthquake of 1978, many buildings were strengthened following the 1977 design guidelines. Most of the damaged buildings had been designed before 1971, when the Architectural Institute of Japan (AIJ) had revised the standard for design of reinforced concrete buildings [8]. Sugano and Endo prepared a review of 157 buildings which had been evaluated and strengthened following the 1977 guidelines [9]. Most of the structures were four stories or less, and over 70 percent were public buildings such as schools or offices. The most common method of strengthening was cast-in-situ concrete walls (45 percent of the cases). Addition of side walls comprised 15 percent of the strengthening cases, while only 1 percent were strengthened by adding steel braces. A majority of these buildings were strengthened before any major earthquake damage had occurred.

One of the few examples of steel bracing used as a seismic strengthening technique was a building at the Tohoku Institute of Technology in Sendai [6,10,11]. The reinforced concrete frame building, constructed in 1968, was damaged in the 1978 Miyagiken-Oki quake. The eight-story building, with three stories below ground, is shown in Fig. 1.6. The major damage occurred in the columns on the north side as shown in Fig. 1.6 (c). The failure in the columns was due to the infilled spandrel walls on the north facade. The spandrel walls gave the north side a stiffness four times greater than that of the other longitudinal frames, so that the north frame attracted a large proportion of the lateral load. In addition, the spandrel walls created "captive" columns which resulted in large shear forces in the columns.

Retrofitting consisted of repairing old elements and adding new ones. The severely damaged portions of columns were removed, additional reinforcement was placed, and the columns were recast. In the transverse direction, some existing walls were thickened, and new shear walls were placed. Eccentric cross braces were installed on both the north and south frames to increase the lateral load capacity in the longitudinal direction. Spandrel walls were cored to reduce their strength and, thus, reduce their ability to generate large shear and flexural stresses in the columns.

The braces were H-sections of weathering steel painted with a rust-stabilizing agent. The same section was used at all levels; however, the braces were weakened at the upper levels to accelerate yielding. Three brace types (B1, B2, B3) were used as shown in Fig. 1.7 (a). Necks near the ends of a brace were produced by cutting holes in the web and outer flange. In addition, the outer flange was cut at the connection point at all levels to produce fully eccentric behavior of the braces. The cuts reduced the stiffness of the steel system, resulting in more evenly matched stiffnesses for the concrete frame and steel bracing.

A post-tensioning technique was used to connect braces to the exterior faces of the beams. Braces were attached by friction bolts to steel bases, which were post-tensioned to the concrete frame by rods passing through holes in the beam, as seen in Fig. 1.7 (b). Mortar filled the gap between the steel base and concrete surface.

Microtremor measurements performed on the completed structure showed that the strengthened building had retrieved its pre-earthquake stiffness. The period of the building in the longitudinal direction was 0.34 sec before the 1978 earthquake, 0.53 sec after it was damaged, and 0.35 sec after rehabilitation. In the transverse direction, the period went from 0.39 sec to 0.43 sec to 0.36 sec after strengthening [10].

Since the steel bracing was a new technique, experiments on the braces, connections, and spandrels were conducted. One-third scale models of the braces were tested under cyclic loading. The ultimate capacity was determined by buckling of the inner flange and web at the necked section. Slip tests on models of the connection at half scale showed that the base-to-beam connection was strong enough to develop the ultimate strength of the braces.

One-third scale tests on the cored spandrel beams indicated that a weakened spandrel had one-third the strength of a regular spandrel for moments producing compression in the region of the holes. Crushing of the concrete around the holes occurred at a lateral load less than that required to produce column shear failure. Therefore, the weakened spandrel beams would fail before the columns and permit development of a ductile failure mechanism.

1.4.3 Japanese Research. As of 1982 over 100 strengthened frames and 40 columns had been tested in Japan. Most of the tests were on one-third scale, single-bay, single-story specimens. More recently three-story frames have been tested. Most of the experiments were on cast-in-place infilled walls using various connection details. Other methods investigated were precast panels, concrete blocks, wingwalls, steel bracing, and steel panels. In Fig. 1.8, Sugano plotted the lateral strength versus displacement relationships for various strengthening techniques and an unstrengthened frame. The data for this graph came chiefly from two series of tests: one conducted by Higashi, the other by Sugano.

Higashi and others conducted tests on fourteen single-bay, single-story frames at one-third scale, in which the columns had poor web reinforcement [8]. Eleven types of strengthening schemes were used in addition to three control frames: two bare frames and one monolithic wall. The three schemes involving steel and the monolithic wall are shown in Fig. 1.9. Other methods included a cast-in-place wall, precast wingwalls, five types of precast walls, and steel plate wrapping of columns.

Cyclic load tests were performed for each test frame. The steel schemes increased the ultimate strength and ductility. In general, though, the initial stiffness of those frames with steel were lower than those with precast panels. The model with precast sidewalls, however, did not show notable increase in strength.

Sugano tested ten one-story, single-bay, one-third scale frames [12]. The nine strengthening schemes, along with the bare frame, consisted of two frames with monolithic walls of different thicknesses, a concrete block wall, two infilled walls with different connections, thickening of a thin wall, a steel panel bolted to the frame, steel compression braces, and tension braces. These frames may be seen in Fig. 1.10 along with their cracking patterns and hysteresis curves. The graph for the unstrengthened frame is at a different scale than the rest of the curves. The H-section compression braces were welded to plates

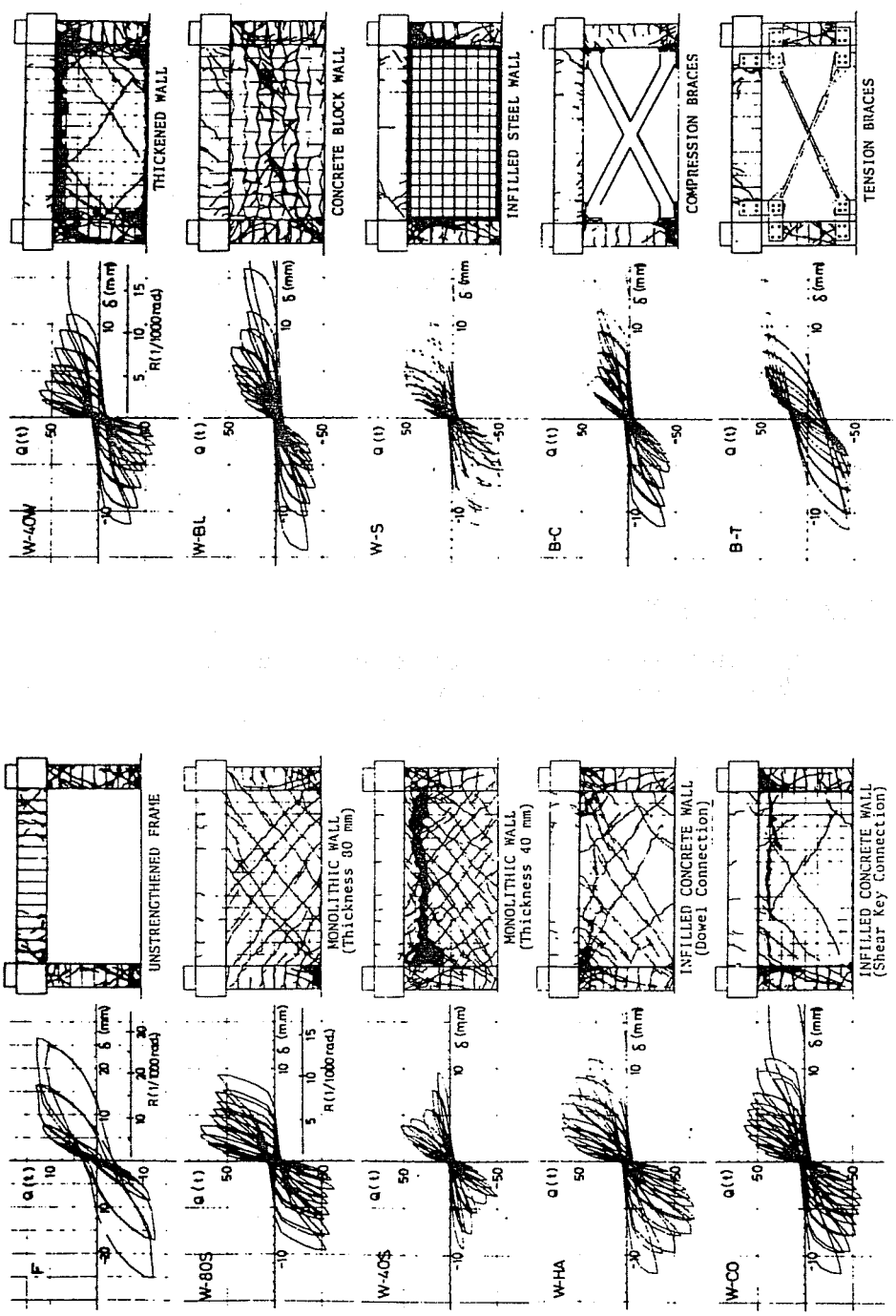


Fig. 1.10 Hysteresis Curves and Crack Patterns for Sugano's Test Frames [12]

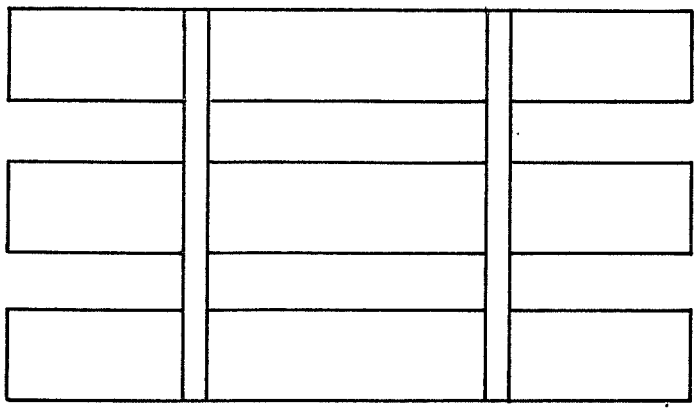

a) Unstrengthened (Bare) Frame

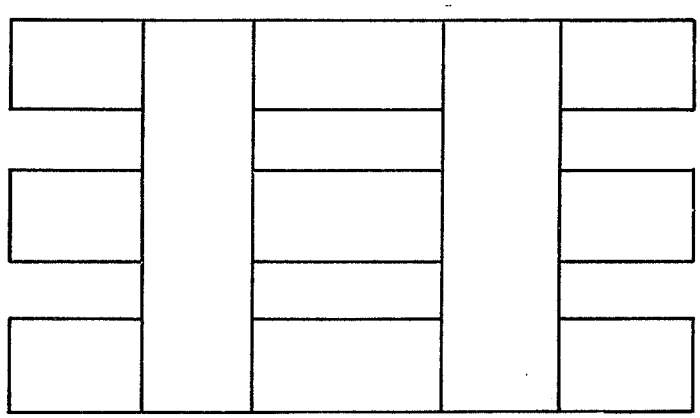

b) Strengthening by Wingwalls

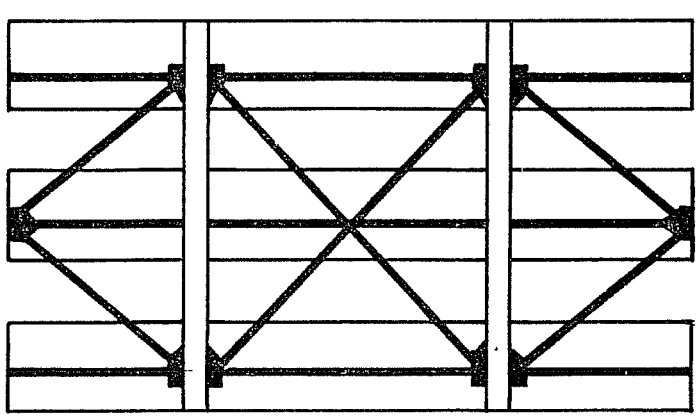

c) Strengthening by Steel Bracing

Fig. 1.11 Three Frame Systems

# CHAPTER 2

# DESCRIPTION OF MODEL

## 2.1. Prototype Building

2.1.1 Description. The prototype for this study is typical of residential and office buildings constructed in California during the 1950's. The seven-story reinforced concrete structure, shown in Fig. 2.1 and Fig. 2.2, has deep spandrel beams and slender columns between the spandrels on the exterior frames in the longitudinal direction. Windows fill the openings between spandrels. A one-way floor slab, 6 in. deep, spans between the exterior spandrels and interior shallow beams, which are not shown in Fig. 2.1 for clarity. All reinforcing steel is Grade 40 except the column vertical steel, which is Grade 60; the specified concrete strength is 3000 psi.

The lateral load resisting system consists of four shear walls in the short direction and the moment resisting frames in the longitudinal direction. The floor slab acts as a diaphragm to distribute the lateral load. Since the interior frames are extremely flexible relative to the exterior frames in the longitudinal direction, the outer frames attract most of the lateral load.

2.1.2 Analysis. Determination of seismic loads and design of the members followed the 1955 Uniform Building Code [13]. Figure 2.2 indicates the disproportionate sizing of the members. The 72 in. by 8 in. spandrel beams with a steel area of 3.84 $in.^2$ are stronger in both flexure and shear than the 18 in. by 18 in. columns with six #10 bars.

The critical section capacity under lateral load is the column shear strength. With a design base shear force of 1064 kips, a column working shear strength of 39 kips, and assuming that only the exterior rows of columns carry the lateral load, the 18 in. columns are inadequate at the first and second levels. In the original design, it could have been assumed that the interior columns helped carry the lateral forces, in which case the columns are adequate. However, it may be unconservative to assign interior columns significant shear considering that the interior beams are only 6 in. deep compared to the 6 ft deep beams on the exterior. The spandrels produce captive columns only 4 ft in height which are almost six times stiffer than the interior columns.

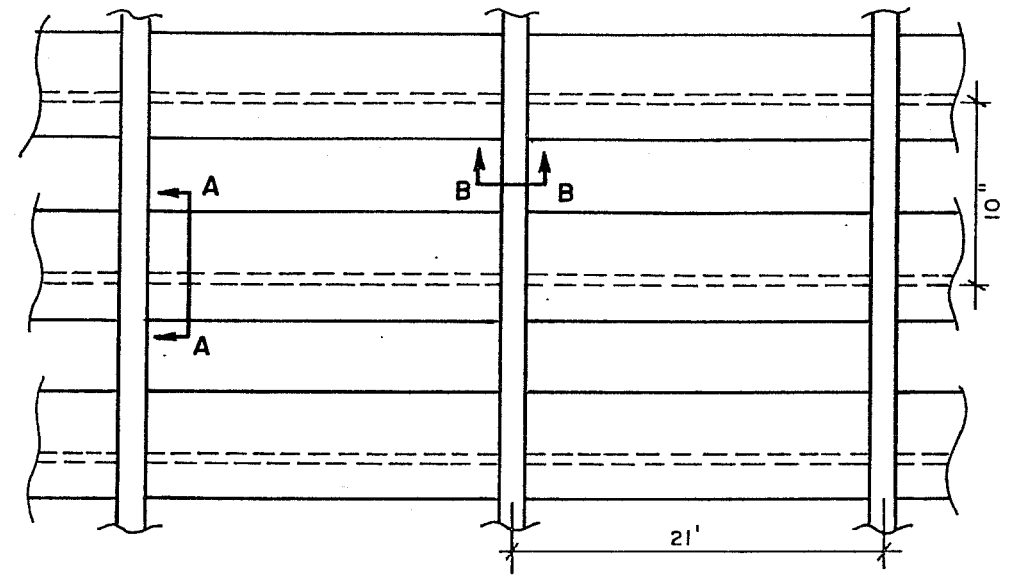


ELEVATION

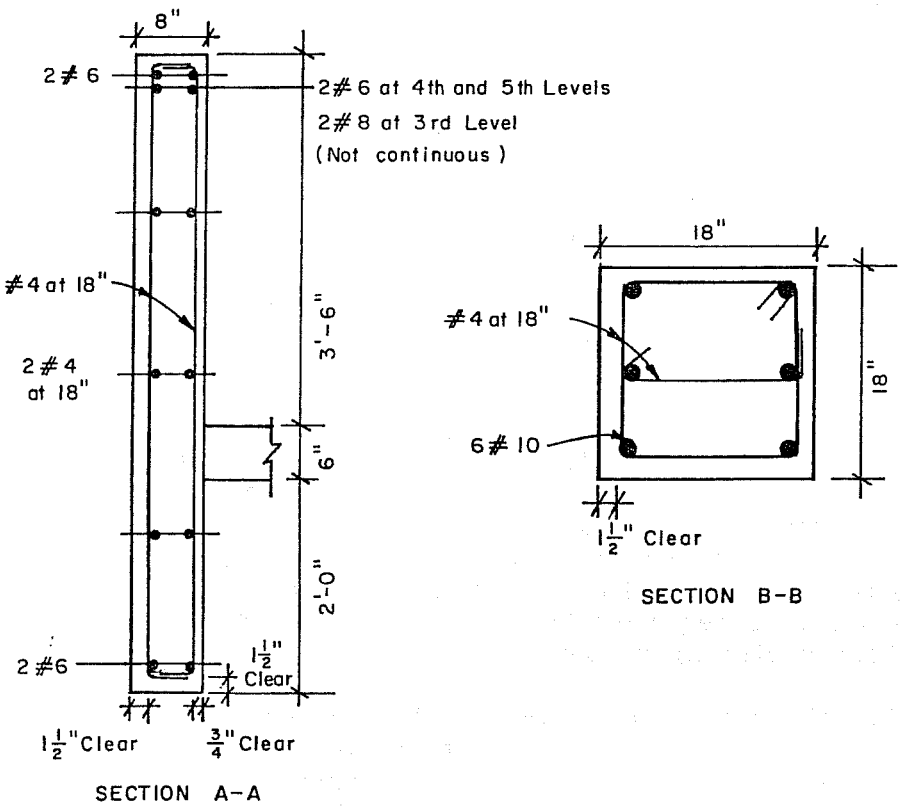


SECTION A-A

SECTION B-B

Fig. 2.2 Prototype Details

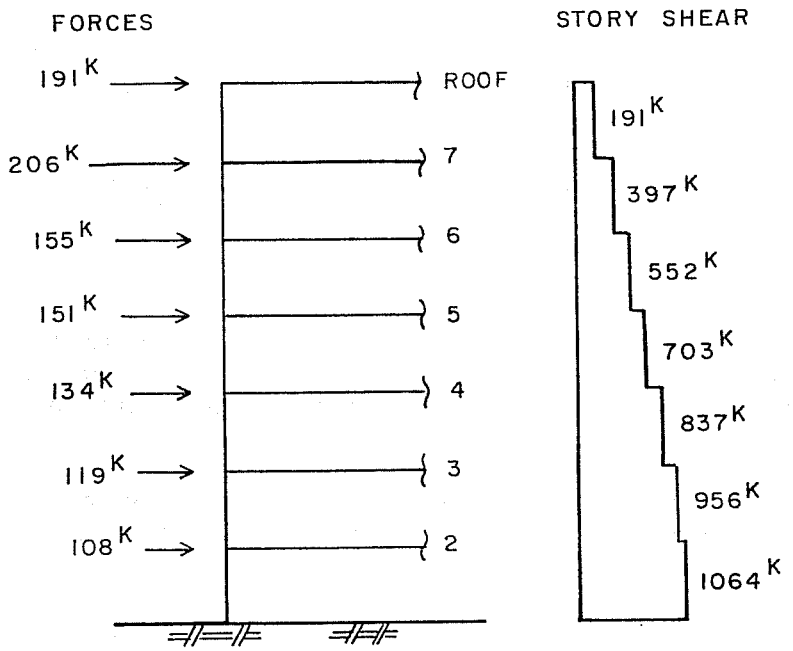


a) 1955 Loads - Entire Building

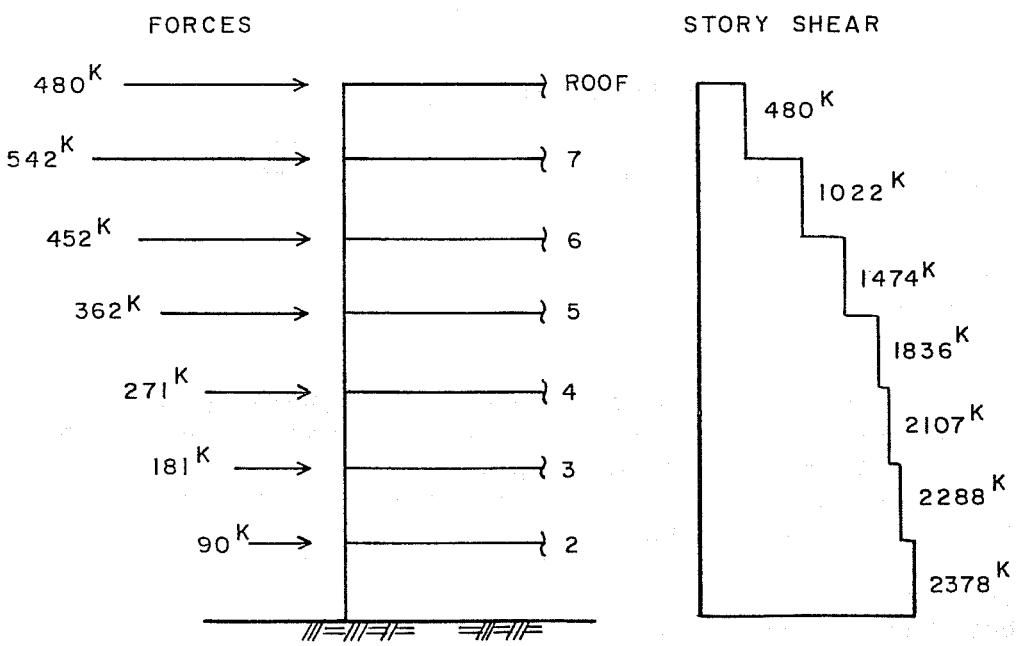


b) 1982 Loads - Entire Building

Fig. 2.3 Comparison of UBC Lateral Earthquake Loads

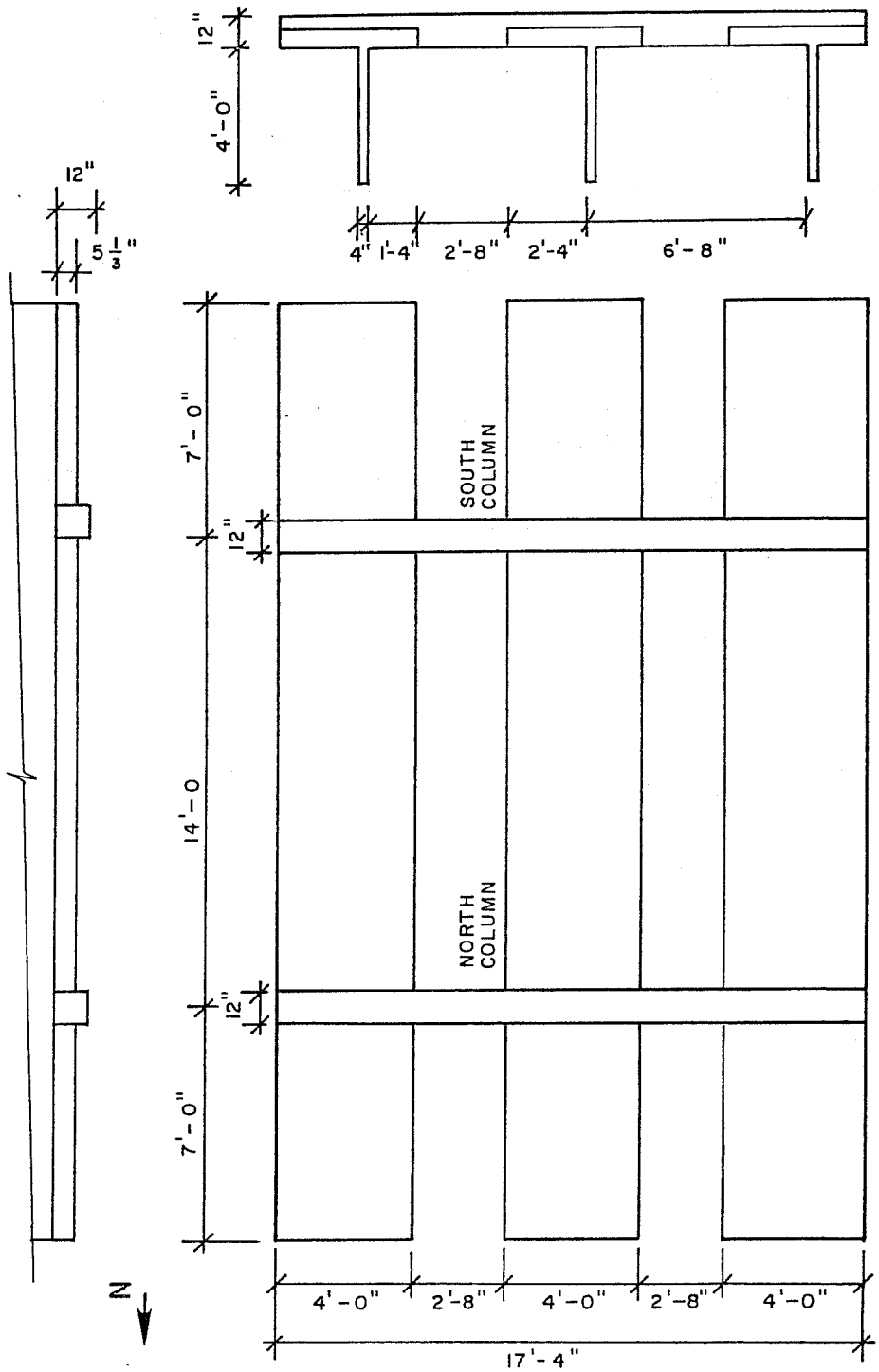


Fig. 2.4 Test specimen dimensions

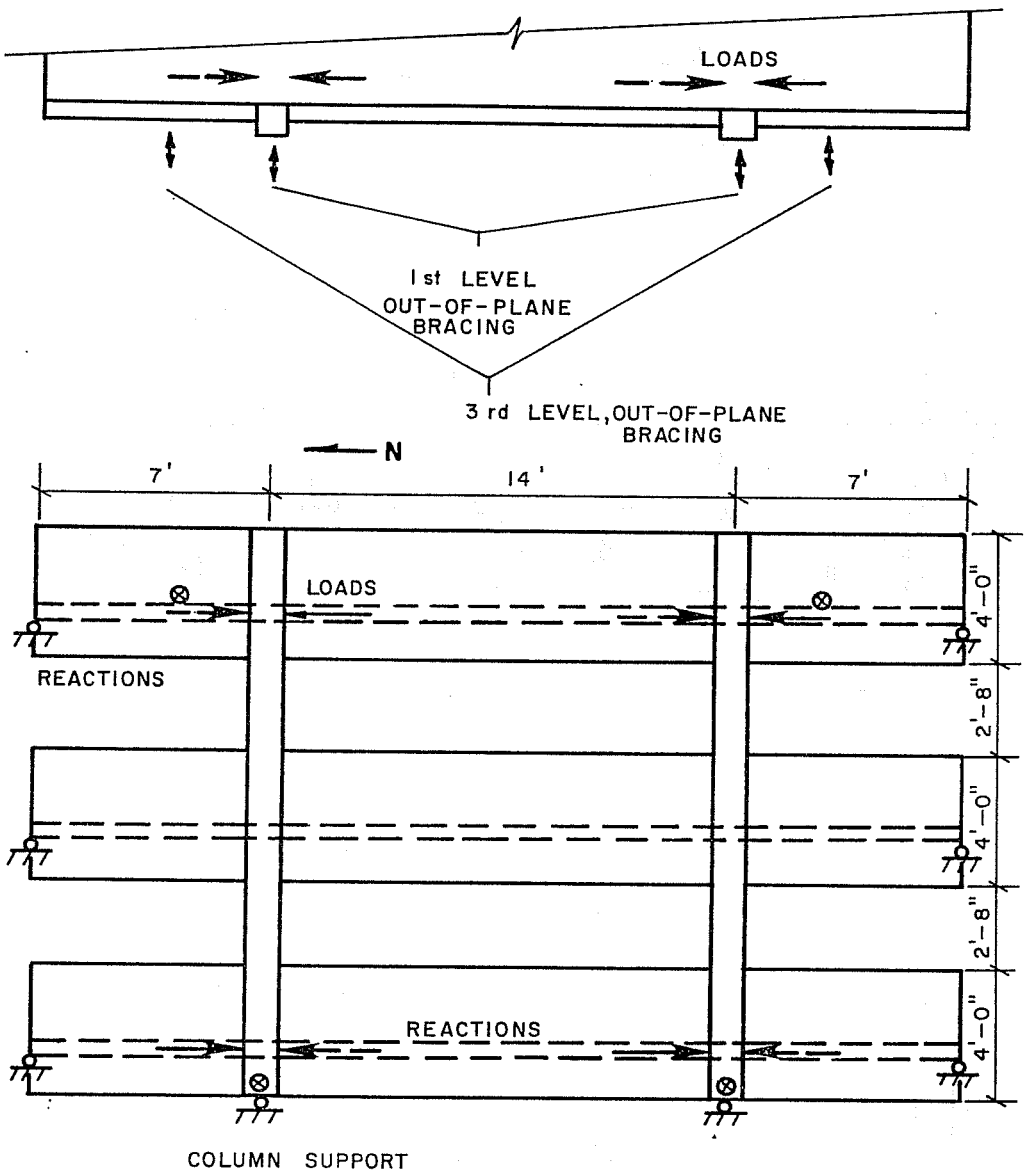


Fig. 2.6 Boundary Conditions of Test Specimen

## 2.4 Steel Strengthening Scheme

2.4.1 Overall Scheme. The strengthening scheme which will be discussed in detail here consisted of exposed structural steel diagonal braces designed to carry the entire lateral load. The bracing scheme, shown in Fig. 2.8, was to be used over eight bays of each of the two exterior frames of the prototype building. The number of braced bays was determined by the criterion that there should be no uplift of the columns due to overturning moments.

The existing concrete building must carry the gravity loads and be able to transfer the lateral loads into the exterior steel. The bracing system picks up the lateral load through steel collectors which are attached, with epoxy-grouted threaded bars, to the outside spandrel faces at the floor levels. Steel columns, attached in the same manner to both sides of the concrete column, were designed to carry the forces produced by overturning moments.

2.4.2 Design of Members. The braces were first designed for the full-scale prototype building to carry the entire seismic shear forces at each story. Earthquake loads for a building in seismic zone 4 were computed following the 1982 Uniform Building Code. Wide flange and structural tube members were considered for the braces. Although tubes are regarded as more architecturally attractive, wide flange members were chosen for easier field erection. The lateral load analysis resulted in 8 in. deep steel braces, collectors, and columns for the prototype.

An important consideration in the design of the steel strengthening scheme was that the loading system in the laboratory would be capable of failing the model braces. The maximum test load necessary to produce failure was computed by assuming that all tension braces yield as the compression braces buckle. The resulting horizontal load was added to the shear capacity of the two concrete columns. To ensure that failure would occur before a maximum lateral force of 400 kips (capacity of loading system) was reached, a value of 330 kips was set as the allowable horizontal load computed for the above failure mechanism.

The original 8 in. deep prototype members scaled down to 6 in. deep model members were too strong. Working in the two-thirds scale sizes, braces were designed which were satisfactory for the scaled-down UBC loads and also led to a horizontal failure load of about 330 kips. Reducing the area of the brace

section decreased the tension and compression capacities for the member, but the braces were still too strong. The radius of gyration about the Y-Y axis, $r_y$, had to be reduced in order to lower the buckling load of the brace. This resulted in fairly large slenderness, or L/r, ratios for the weak axis.

All 5 in. and 6 in. deep standard wide flange sections were too large. Rather than fabricate suitable wide flange sections from rolled plates, a standard W6X9 section was modified by removing the tips of the flanges along the length of the brace resulting in a 3-1/2 in. flange width. This reduced section has an L/r ratio of 140.

For the original prototype bracing system, design requirements were set which included limiting the effective slenderness ratio, KL/r, to 100 and preferably less than 80. The values were chosen in reference to steel strut tests performed at the University of California at Berkeley [16], where eighteen struts with three effective slenderness ratios (40, 80, 120) were tested under reversed cyclic loads. The specimens with lower KL/r values produced "fatter" hysteresis loops, indicating better energy absorption. The struts with an effective slenderness ratio of 120 had steep load-deflection curves which showed substantial deterioration of peak compression loads with each cycle.

For the pure fixed-fixed end condition (K=0.5), the modified W6X9 braces for the model have an effective slenderness ratio of 70; using the design K-factor of 0.65 yields a ratio of 91. Although the L/r ratio of 140 is high, the end restraints yield a reasonable effective slenderness ratio and satisfactory hysteretic performance. In the calculations for the expected peak capacity, it was recognized that Grade 36 steel can have a yield strength as high as 45 ksi. At a yield stress of 45 ksi, the tension capacity of one brace is 109 kips, and, with a K-factor of 0.5, the buckling load of one brace is 88 kips. Adding the horizontal components of the loads in two tension braces and two compression braces to the shear capacity of two concrete columns (63 kips) yields a lateral failure load of 338 kips. It must be noted that this estimate neglects the shear strength of the steel columns and their interaction with the concrete columns.

The steel columns and collectors in the model were each designed following two criteria. First, they had to be able to carry the forces which would be produced by the model braces at their ultimate capacity. Second, they were checked under allowable stress design using scaled-down loads from the UBC.

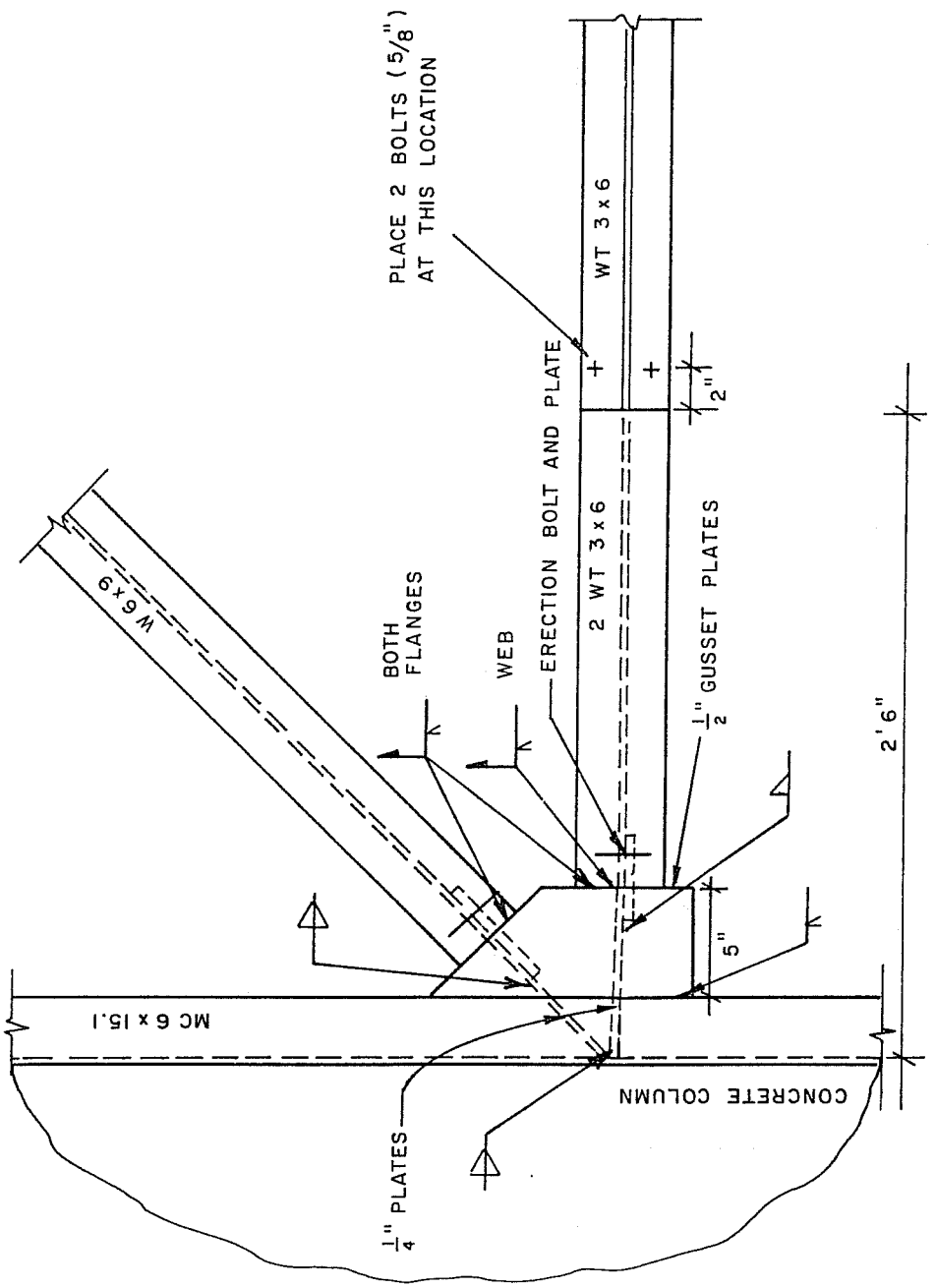


Fig. 2.9 Brace-to-Channel Connection

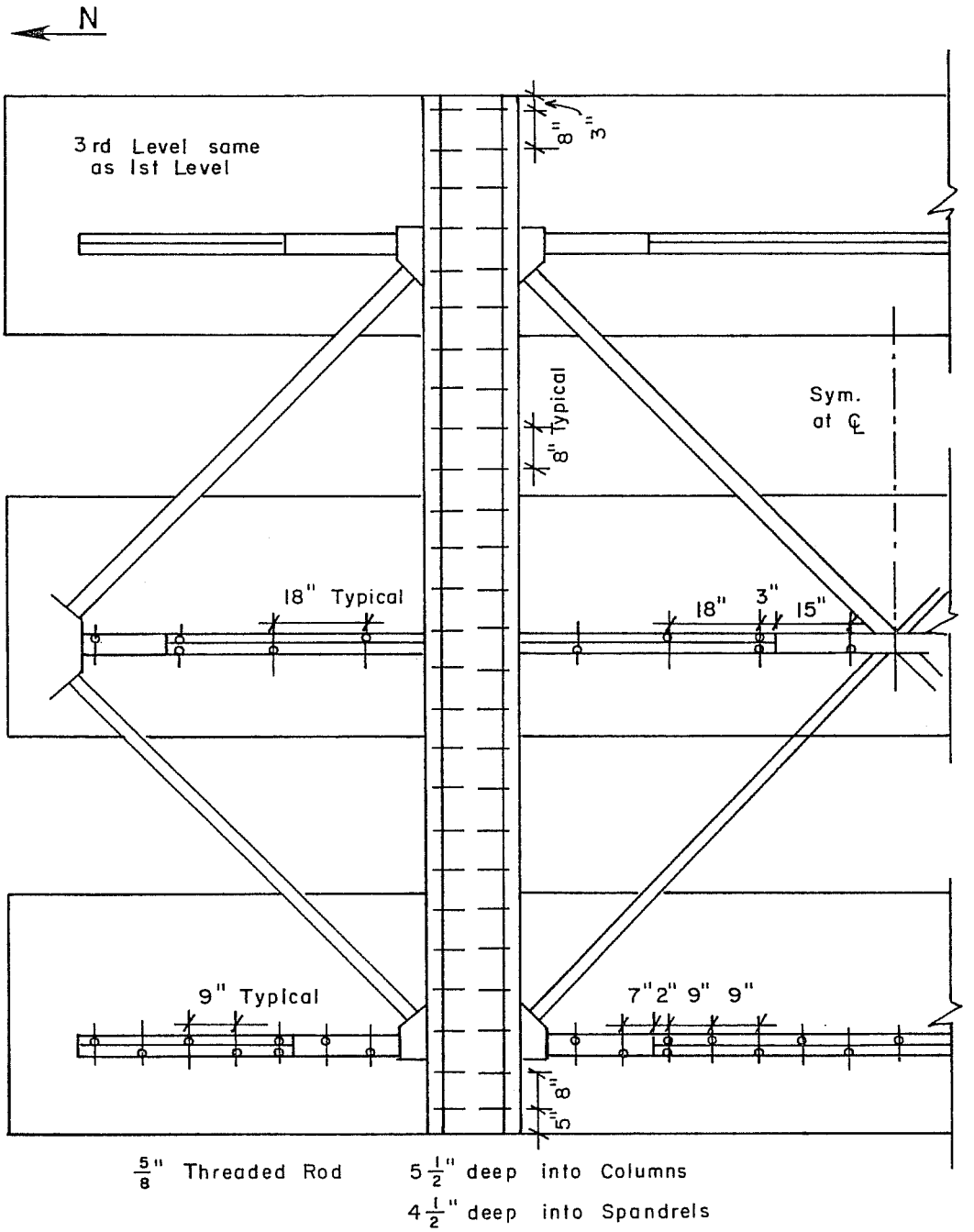


Fig. 2.11 Dowel Layout

# CHAPTER 3

## EXPERIMENTAL PROGRAM

### 3.1 Construction of Original Frame

3.1.1 Procedure. The construction of the bare frame was carried out in six stages as seen in Fig. 3.1. The bottom of each spandrel up to the top of the floor slab was cast in one stage, while the upper portion of each spandrel and the columns above (up to the next spandrel) were cast in the next stage. Formwork for the exterior of the spandrels was continuous over the full 4 ft height; therefore, forms for the lower portions of the spandrels and the slab were left in place when the upper portions of the spandrels were cast. After the second and fourth casts, forms were stripped, cleaned and erected for the next levels.

Figures 3.2 through 3.7 are photographs of the construction procedure. The slab and inside spandrel forms for the first level are shown in Fig. 3.2. These forms are in six units to allow for easier removal and for differences in slab depth described later in this chapter. Each unit consisted of the slab formwork supported by shoring and forms for the lower inside face of the spandrel, which rested on a base 4-1/4 in. above the lab floor. Neoprene pads formed the base of the columns.

The spandrel reinforcement cages were set in place on the base in two halves and spliced in the middle. The forms for the exterior of the spandrels (in four units) were set on the base, and the thickness of the spandrel was achieved using formties. The column bars (extending 18 in. above the slab) and ties were threaded into position, and the exterior column form was placed on the base. The formwork for the exterior face of the columns was bolted to the spandrel forms and extended to the bottom of the next spandrel beam. The slab steel reinforcement was placed, and the first level was cast up to the top of the slab.

For the next stage, the column exterior forms were removed to allow for the column cages to be fabricated. The vertical bars were spliced just above the slab at each level. The forms for the inside face of the spandrel were set on the concrete slab and held at the correct distance from the exterior forms with formties. Figure 3.3 shows the spandrel forms and

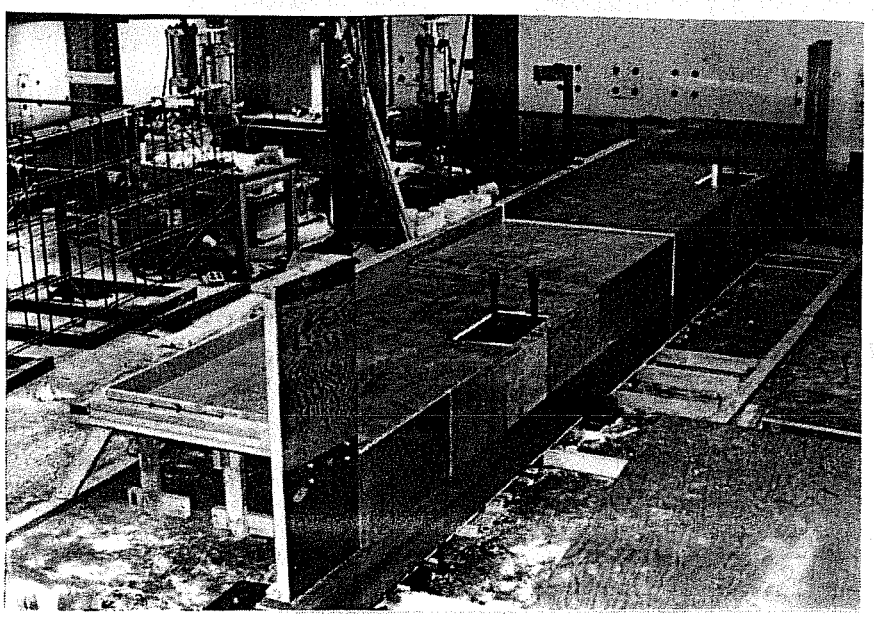

Fig. 3.2 Slab forms at first level

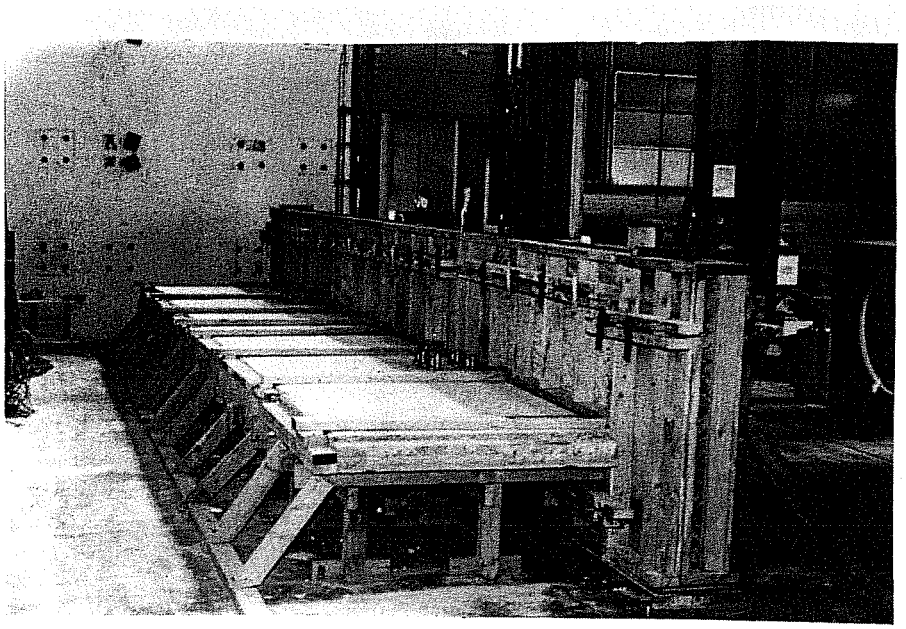

Fig. 3.3 Spandrel forms in place for second cast

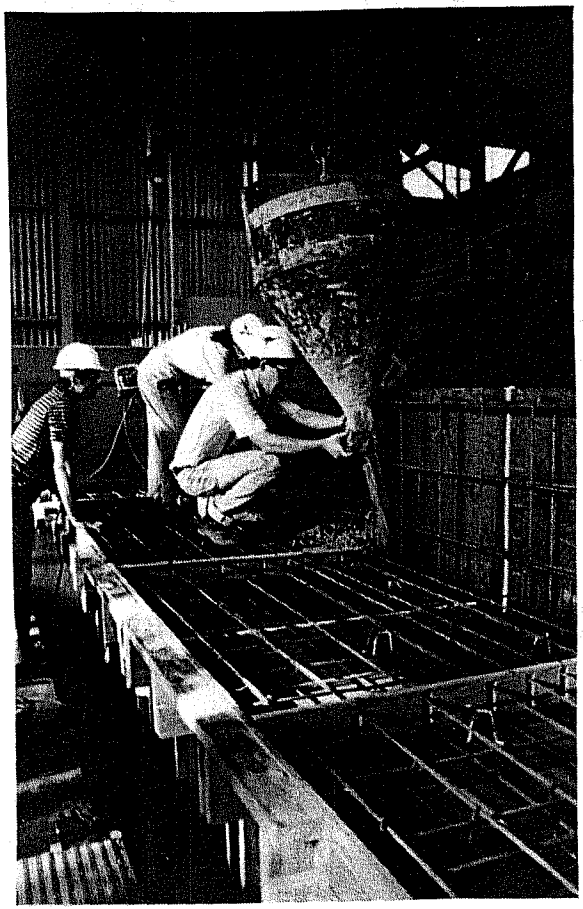

Fig. 3.6 Casting third level slab

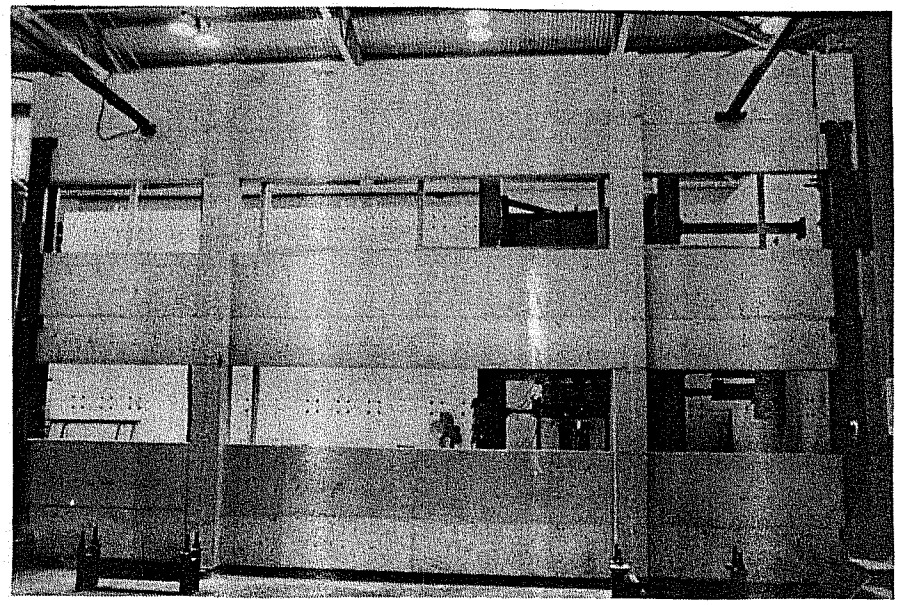

Fig. 3.7 Bare frame

TABLE 3.1 Concrete Mix Proportions

| Component | Quantity per Cubic Yard |
|---|---|
| Cement (Type I) | 423 lbs |
| Gravel (maximum aggregate size = 3/4") | 1735 lbs |
| Sand | 1360 lbs |
| Water | 30 gals |
| Water-Reducing Admixture | 13 ozs |
| Air-Entraining Admixture | 3 ozs |

TABLE 3.2 Concrete Strength
(Avg of 3 cylinders)

| Casting Stage | $f'_c$ - 28 days (psi) | $f'_c$ - time of test (psi) |
|---|---|---|
| 1 | 4100 | 3930** |
| 2 | 4560 | 4730 |
| 3 | 4350 | 4630 |
| 4 | 3730 | 4360 |
| 5 | 2580 | 3010 |
| 6 | 5450* | 5790 |

*at 47 days
**Avg. of 2 cylinders

Several changes were made to accommodate the vertical struts at the ends of the spandrels. The length of the frame was increased at each end by 8 in. to allow vertical restraints to be located at what would be the center of the side spans. The floor slab was terminated 16 in. short of the spandrel end at all levels to allow space for the vertical strut members. The bottom corners of the first level spandrel were blocked out to leave clearance for the base fixtures of the struts.

To provide sufficient shear and bearing at the points of application and horizontal restraint in the floor slab, the slab thickness was increased in the regions around the columns at the first and third levels. The 5 ft wide drop panels were 6 in. deep as Fig. 3.8 shows. In addition, more slab reinforcement was placed in the drop panels, as indicated in Fig. 3.9. Typical slab reinforcement in the short direction consisted of #3's at 8 in. with 90 degree hooks into the spandrel, and, in the long direction, #3 bars on 4 in. centers near the spandrel and 8 in. centers elsewhere. For the drop panels, the spacing of the #3 bars with hooks was decreased to 4 in. The two layers of longitudinal #3 bars passed through the drop panel except for the three bars closest to the spandrel. These top bars were spliced to three #6 bars within the drop panel. Three #6 bars formed the bottom layer of reinforcement in the drop panel near the spandrel; #3 bars with 90 degree hooks on the ends were arranged throughout the remainder of the drop panel.

In addition to the steel reinforcement, structural steel members were placed within the column slab joint. Because the centerline of the forces and reactions was 15-1/2 in. from the center of the columns, structural steel was required to carry the torsion produced by the eccentricity of the load and to stiffen the connection. A 6X6X1/2 structural tube, 19 in. long, was embedded in the concrete slab perpendicular to the column and passed about 4 in. into the column, as shown in Fig. 3.10. An 8X18.75 channel section, 28 in. in length, was welded to the tube and was oriented vertically in the column. Holes were drilled in the tubes, through which the #6 reinforcing bars could pass. The #3 bars were butted against the tube.

3.2.2 Application of Load. Figures 3.11 through 3.15 show the loading frame on the third level and the connection to the lab reaction wall. The orientation of the test specimen with respect to the reaction wall is seen in Fig. 3.11. Schematics in Figs. 3.12 and 3.13 and the photo in Fig. 3.14 show the loading frame, which consists of two 6X4 structural tubes connected by 6X6 tubes. The centerhole rams, each with a capacity of about 200 kips and 10 in. travel, are arranged so that two rams apply

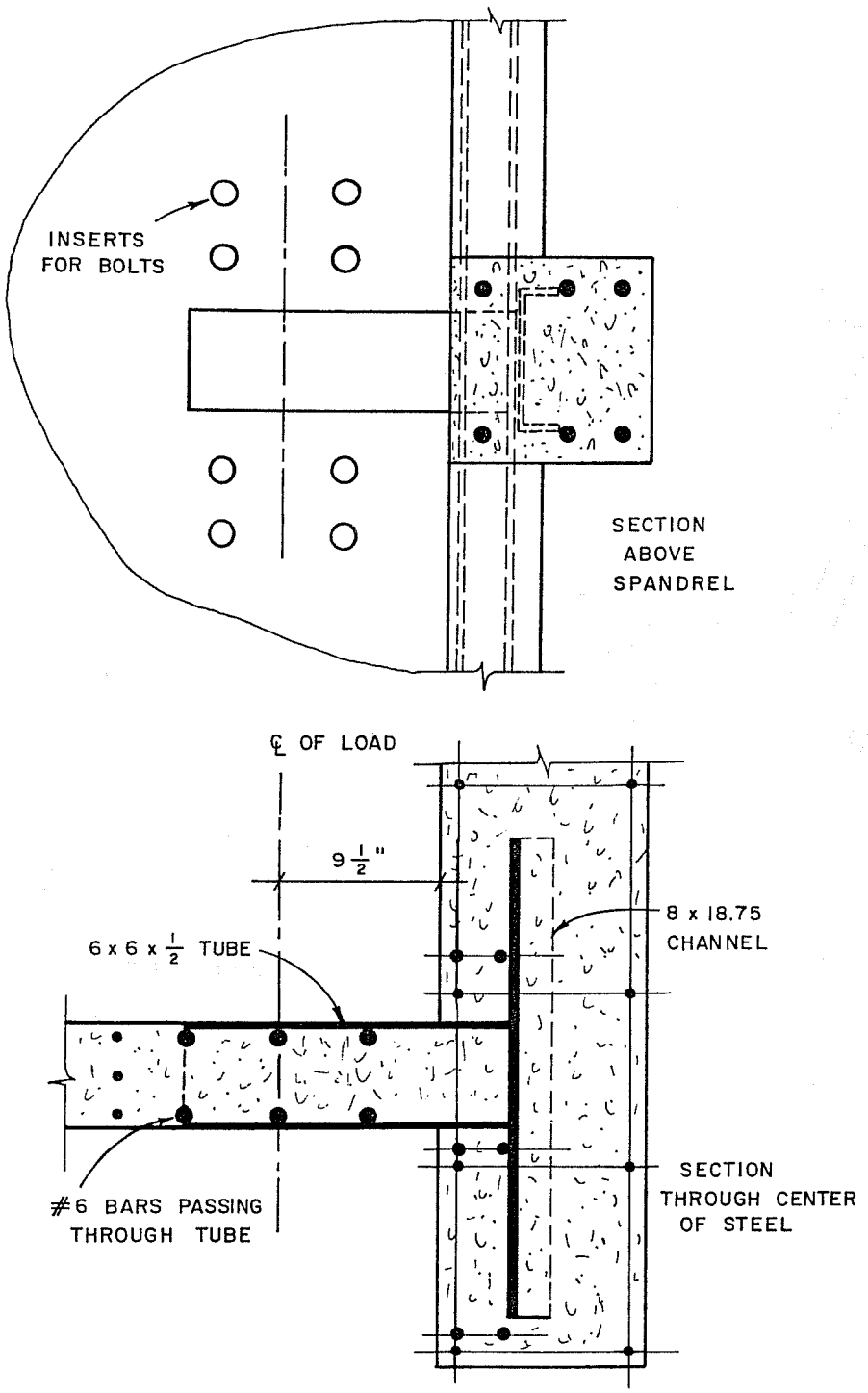


Fig. 3.10 Structural Steel in Column-Slab Joint

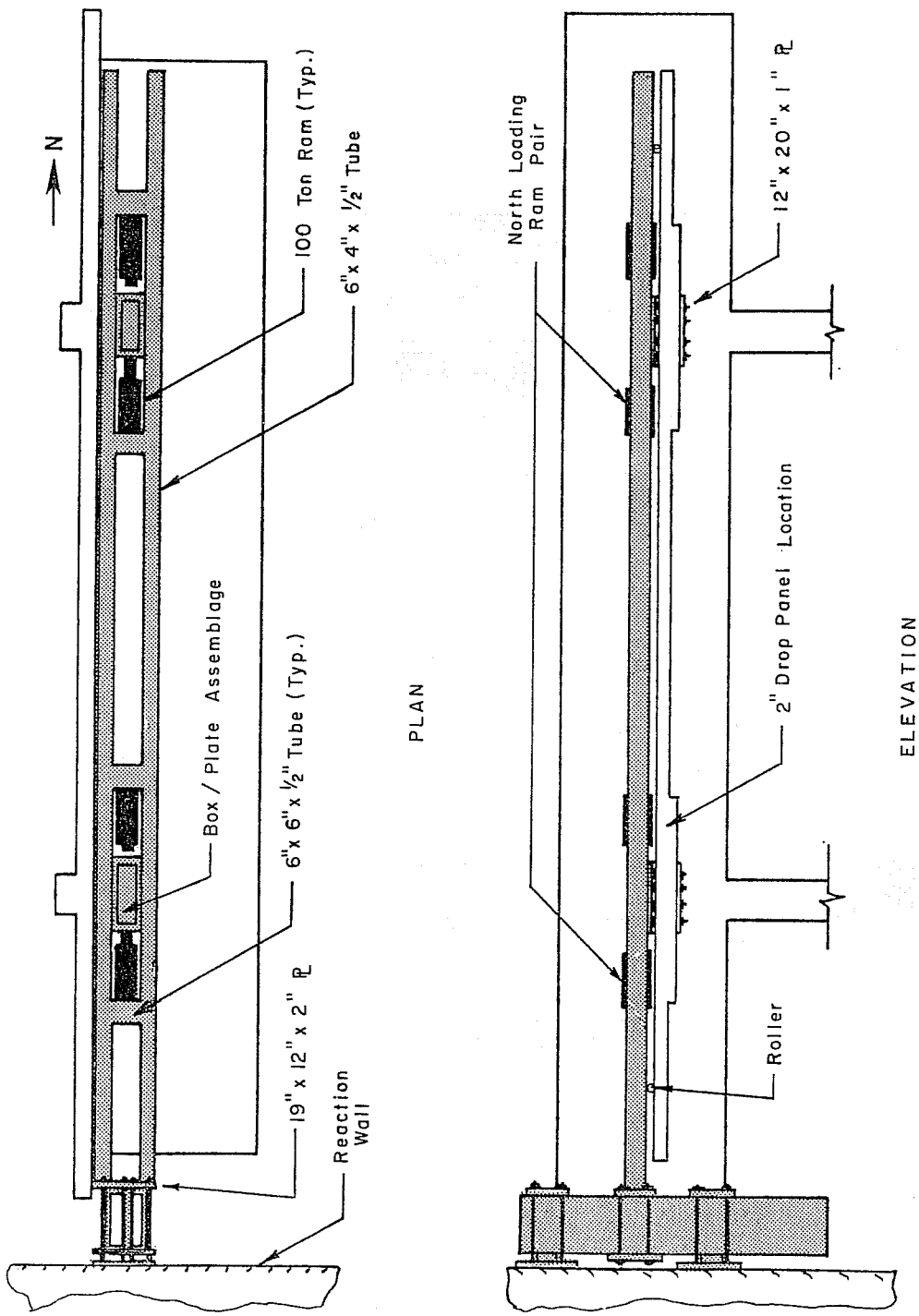


Fig. 3.12 Loading frame

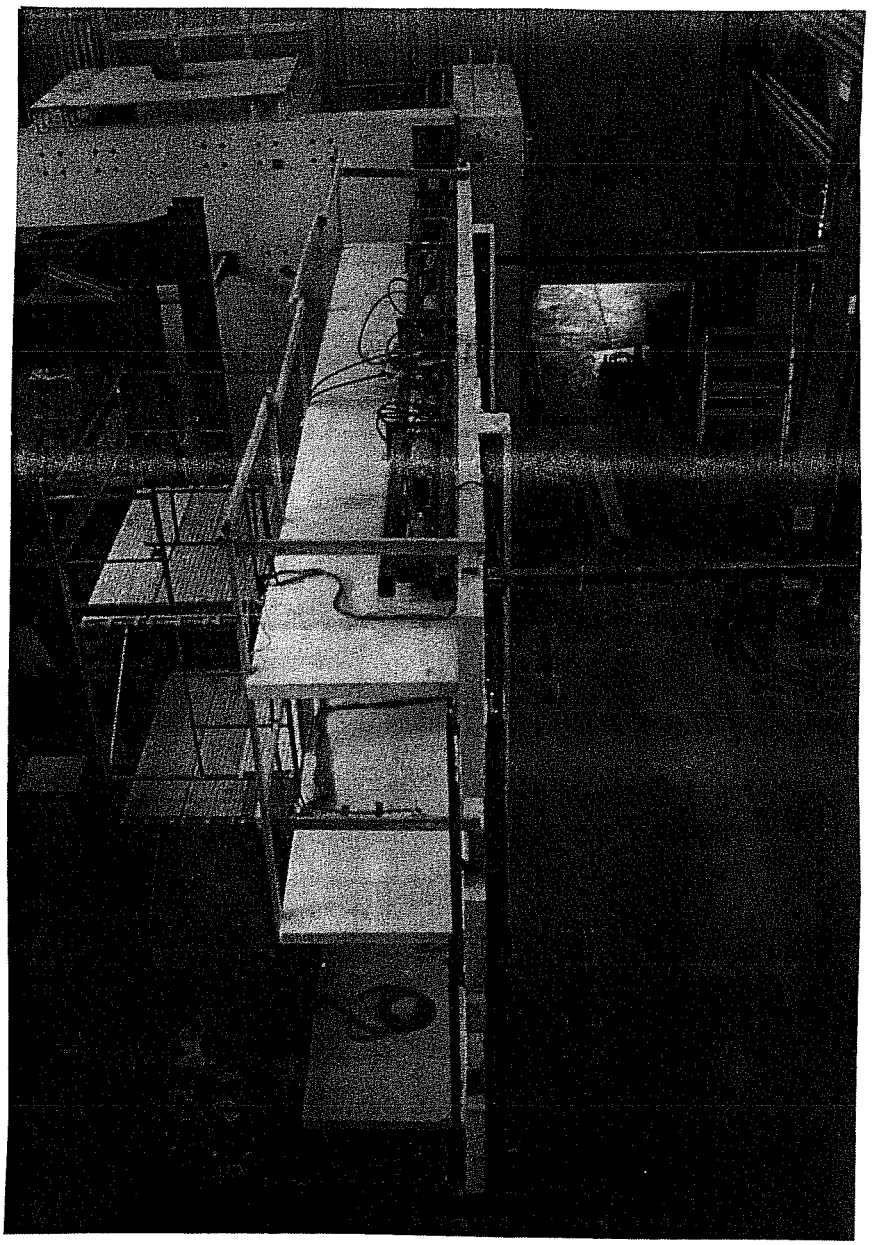

Fig. 3.14 Loading frame at third level slab

load in the north direction (one at each column), and the other two rams in the south direction.

Load was transferred to the slab through a 1-1/4 in. steel plate grouted to the concrete and held by eight 1-1/4 in. high-strength bolts. Each bolt was stressed to 90 kips to develop sufficient friction between the steel plates and concrete floor slab. A Grade 50 steel box section was welded to each 1-1/4 in. plate, and the rams acted against the box. Figure 3.13 shows the arrangement of plates, rams, and bolts.

The rams were placed in the spaces between the 6X6 tube and the box/plate assembly. Pins welded to the box and tube held the centerhole rams at the correct height and prevented them from slipping during testing. Hydraulic lines ran from the rams to a manifold where the loading directions were controlled by hand operated valves.

The two 6X4 tubes on the third level framed into a pair of 18 in. deep channels fastened to the reaction wall. When the specimen was loaded north, the force was transferred to the wall by bearing. For load in the south direction, eight high-strength threaded rods carried the reaction to the rear of the buttress where the force was applied through bearing to the surface of the buttress. Figure 3.15 shows the tension ties passing through the reaction wall to the rear of the buttresses.

3.2.3 Base Reactions. At the first level, the details at the reaction points were very similar to the loading points at the third level. Two plates were clamped to the slab with eight bolts stressed to 90 kips each. The bottom 1-1/4 in. plates were actually tee sections fabricated of Grade 50 steel with a 2 in. pin passing through each tee.

Figure 3.16 shows the two links (5-1/4 in. by 1-1/2 in. Grade 50 steel bars) pin-connected to the tee and to two C15X40 channels anchored to the reaction floor. The links were instrumented to permit measurement of the reactions. The links prevented development of vertical reactions at the reaction points. The channels were grouted to the floor for a better friction surface, and eight bolts at each column were stressed to 50 kips each in order to transfer the load to the lab floor through friction.

3.2.4 Vertical Reactions. Vertical movements at the spandrel ends were restrained by structural steel struts fastened to the reaction floor. The struts for the bare frame and concrete strengthening tests are shown in Fig. 3.17. Eight inch

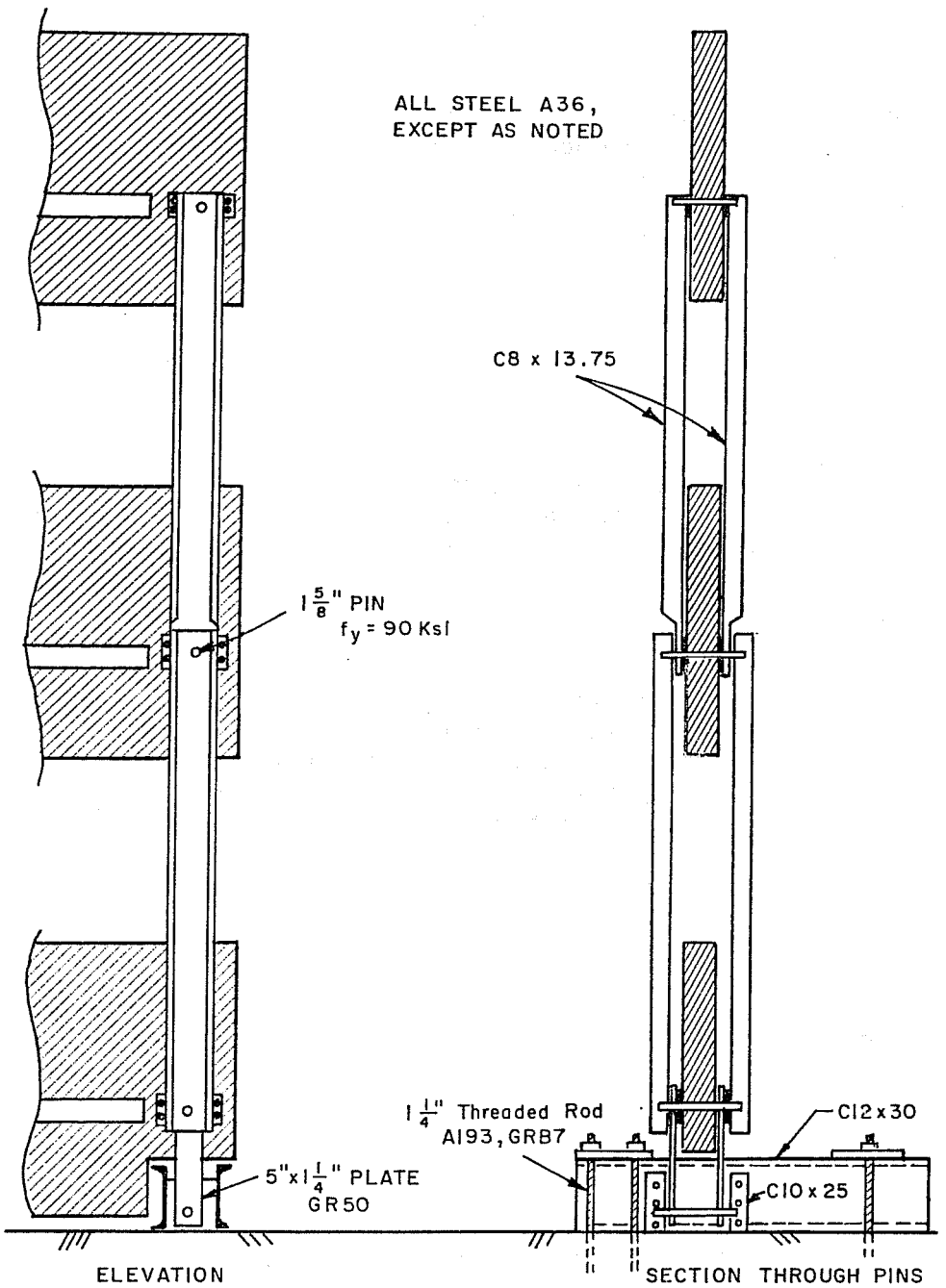


Fig. 3.17 Original Strut Design

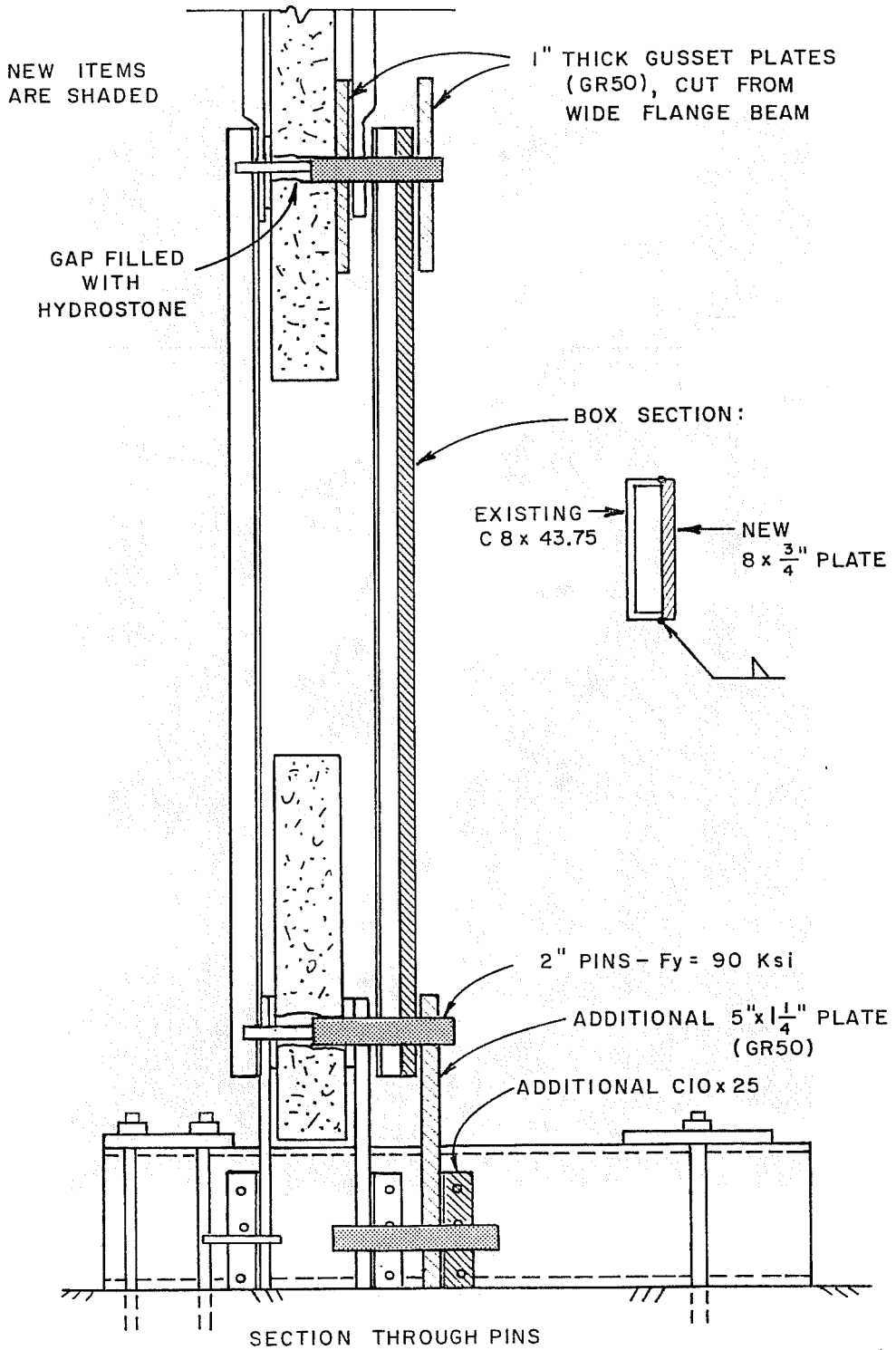


Fig. 3.18 Modifications to Struts

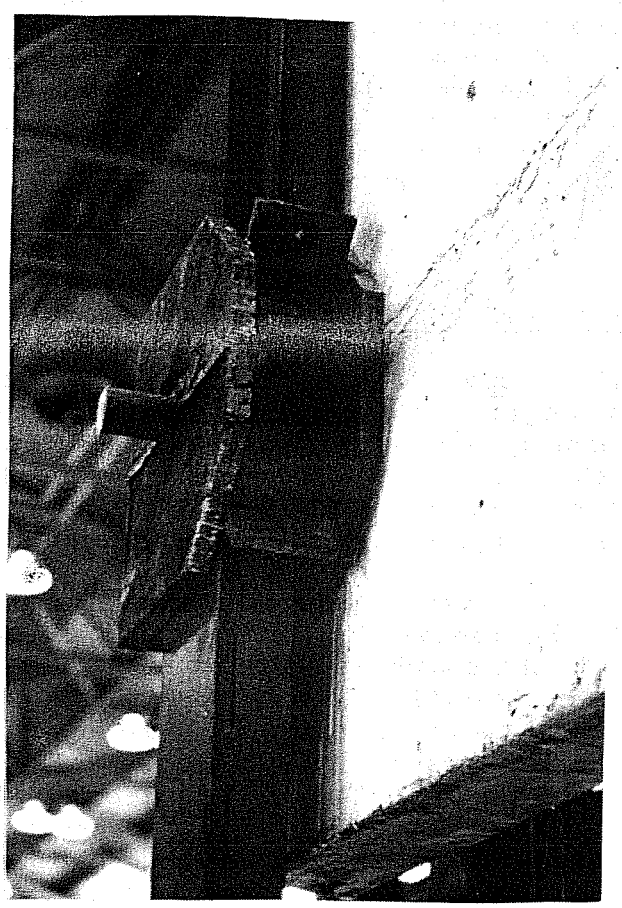

Fig. 3.20 Struts with gusset and erection plates for braces

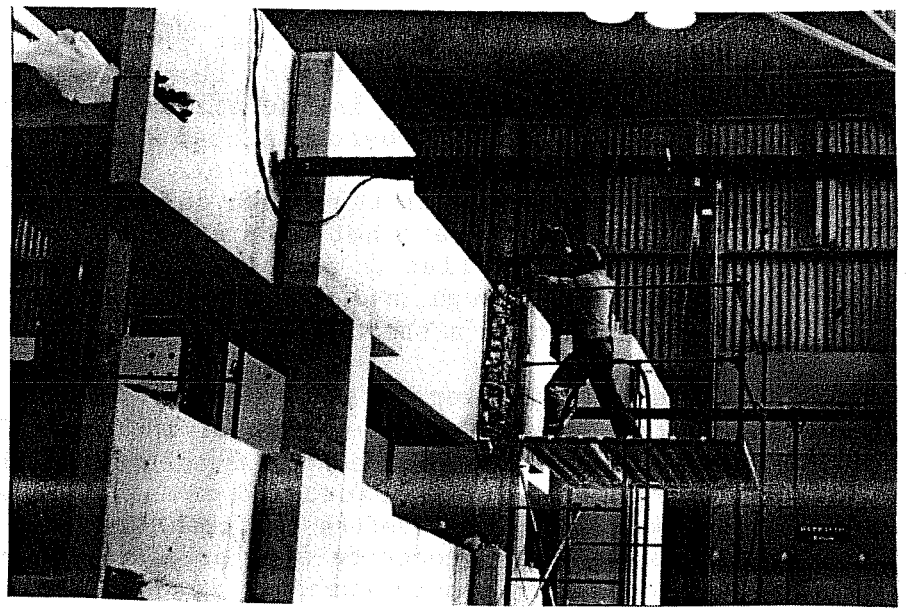

Fig. 3.21 Concrete removal

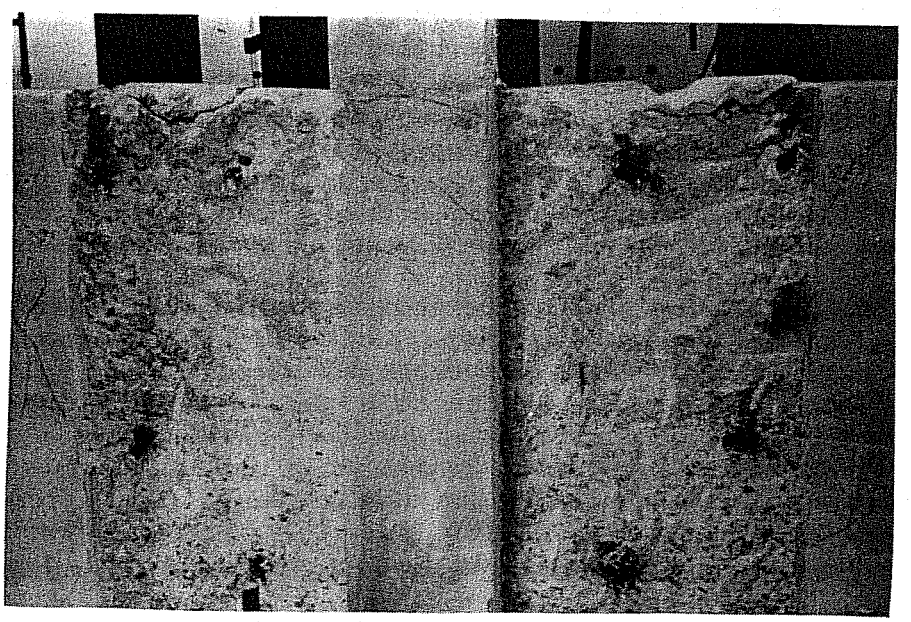

Fig. 3.22 Rough surface around column


Fig. 3.23 Epoxy application procedure

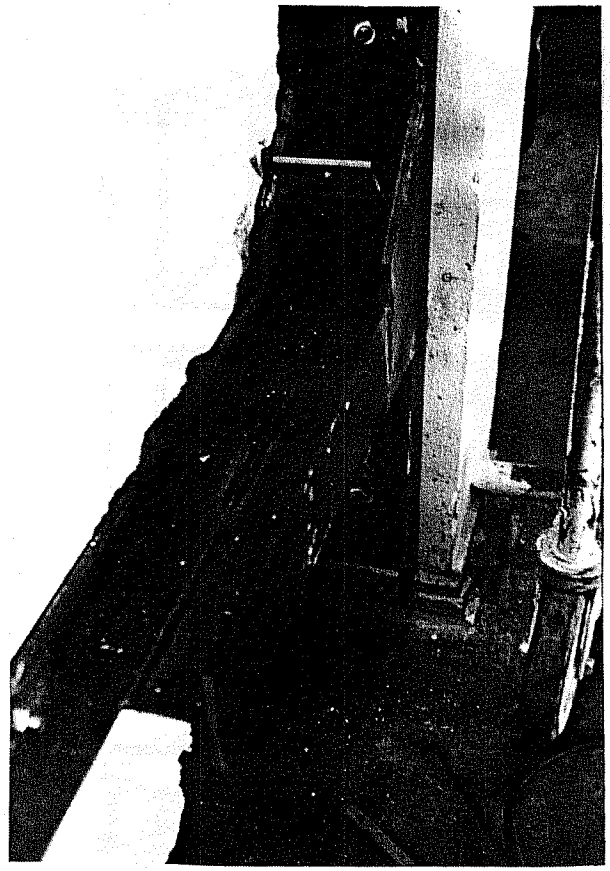

Fig. 3.24 Double tee

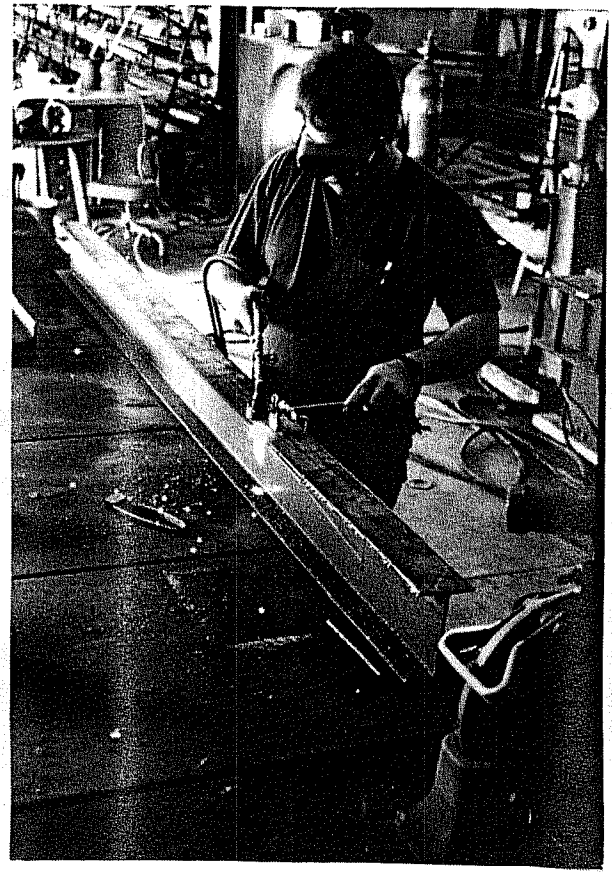

Fig. 3.25 Torch-cutting braces

concrete, and yet was light enough to contrast with the original steel color. The paint indicated steel yielding during the test because it flakes off with the brittle mill scale when the steel beneath is yielding.

3.3.4 Materials. The tees, channels, and wide flange members were Grade 36 steel. Mill reports were obtained from the supplier for the W6X9 braces, which showed an average yield strength of 48.1 ksi.

To verify the figures from the mill reports, tension tests were carried out on samples obtained from extra brace material which came from the same heat. Four coupons were tested (two from the web, two from the flange) following the specifications in ASTM 370-71 [21]. The average static yield values were 48.8 ksi for the web material and 44.5 ksi for the flanges.

Threaded rods and nuts for the dowels were mild steel. High-strength washers were used because their dimensions met clearance requirements on the tees. All welds were formed with either E60-13 or E70-18 electrodes.

## 3.4 Instrumentation

3.4.1 Loads. The lateral load applied at the third level was measured through use of a pressure transducer. One transducer located at the pump measured the pressure in the hydraulic lines, whether loading the frame north or south. The applied load, then, was the line pressure times the piston area of two rams.

The horizontal reaction forces at the base and the vertical reactions in the end struts were measured by load cells made up of four or eight strain gages. The gages were arranged on the links and struts to increase the sensitivity of the four arm bridge load cells. Each base reaction was measured using the two horizontal links, which had eight strain gages (four on each link) making up the load cell.

The vertical reactions were measured at each level at both ends for a total of six reaction forces. For the original frame test, each pair of struts with eight gages formed a load cell. Only the pairs between the second and third levels were retained as they were for the steel strengthening test. At the bottom level, the plate on the interior of the spandrel at each

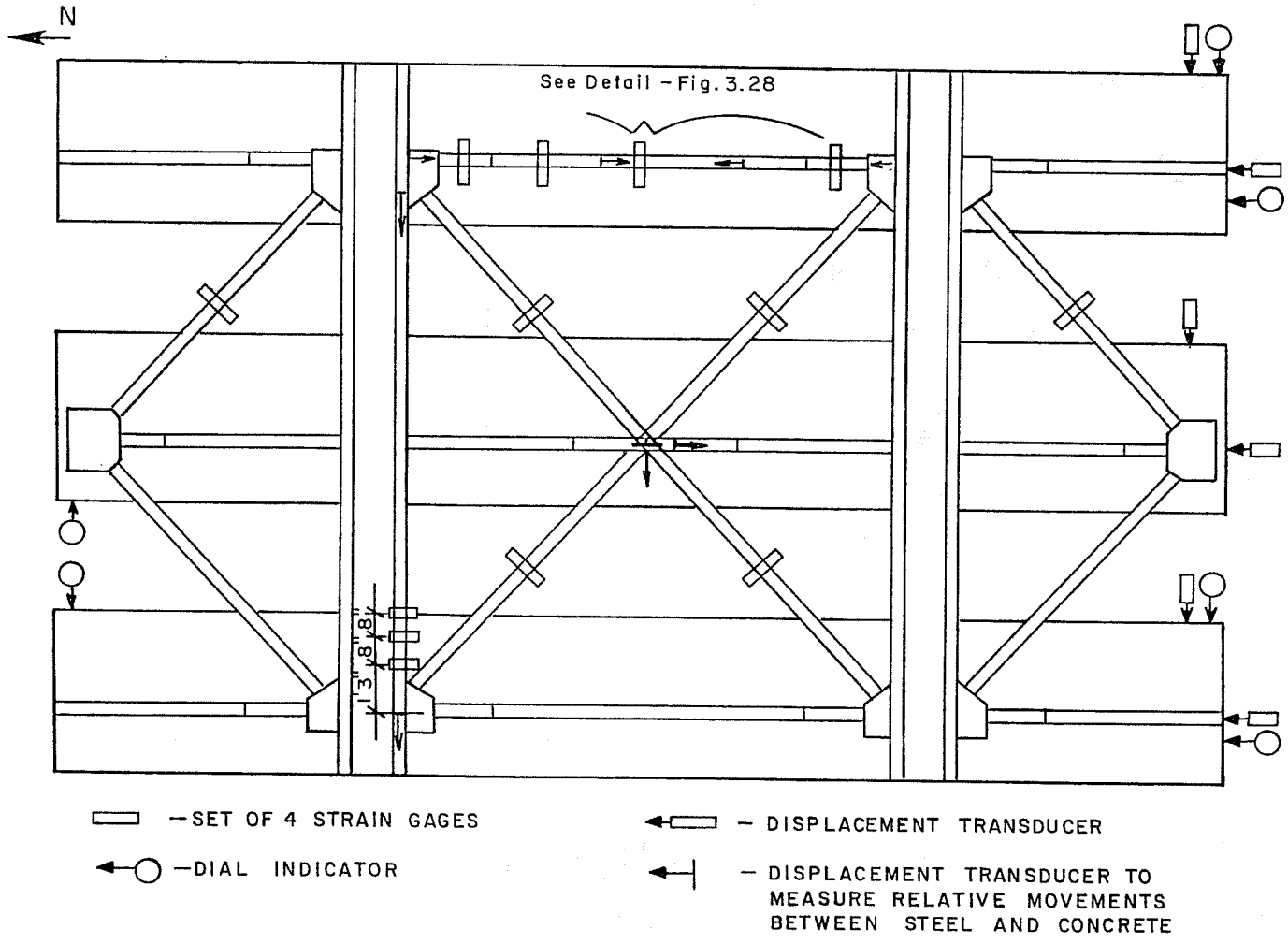


Fig. 3.27 Instrumentation Locations

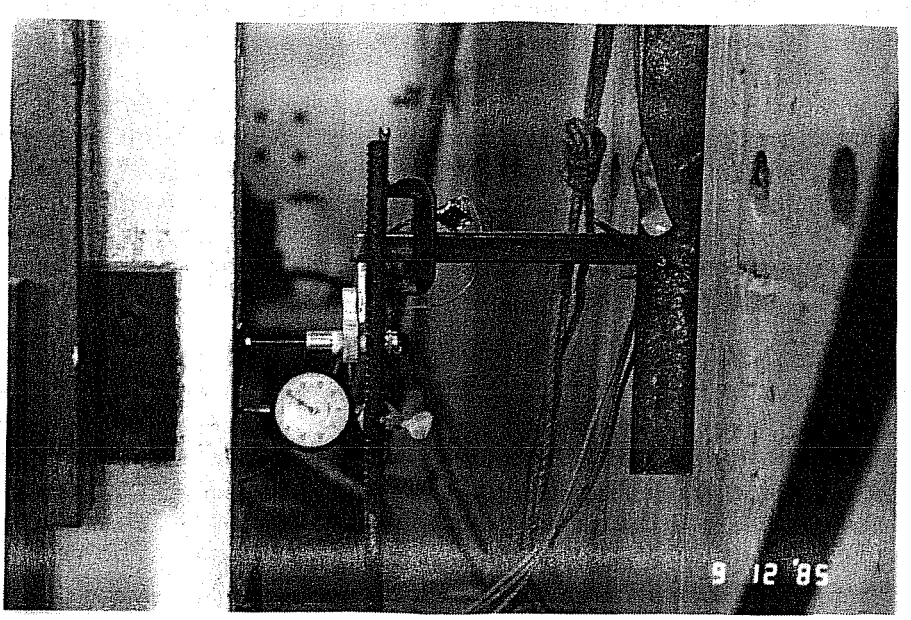


Fig. 3.29 Transducer and dial gage at first level

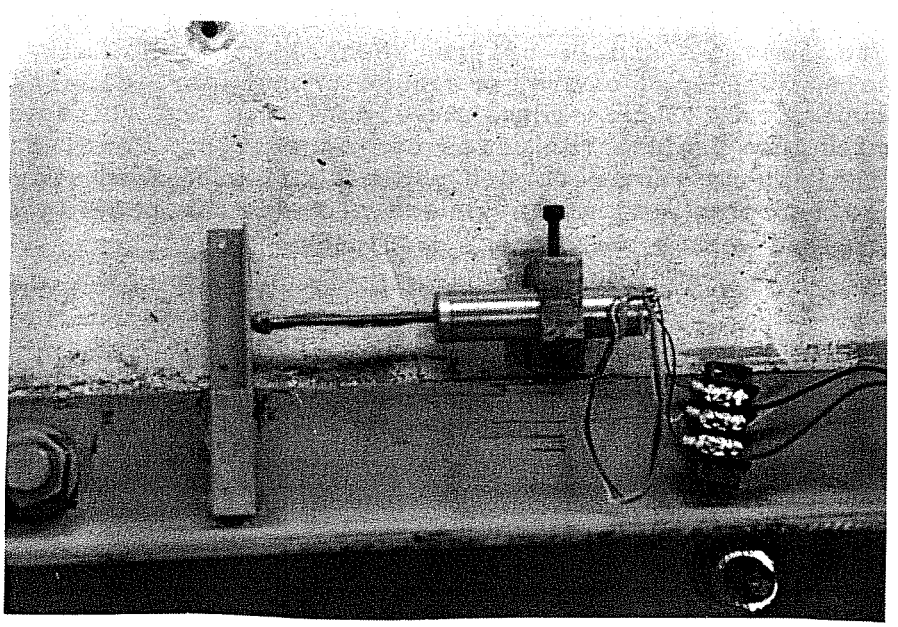

Fig. 3.30 Transducer measuring tee movement

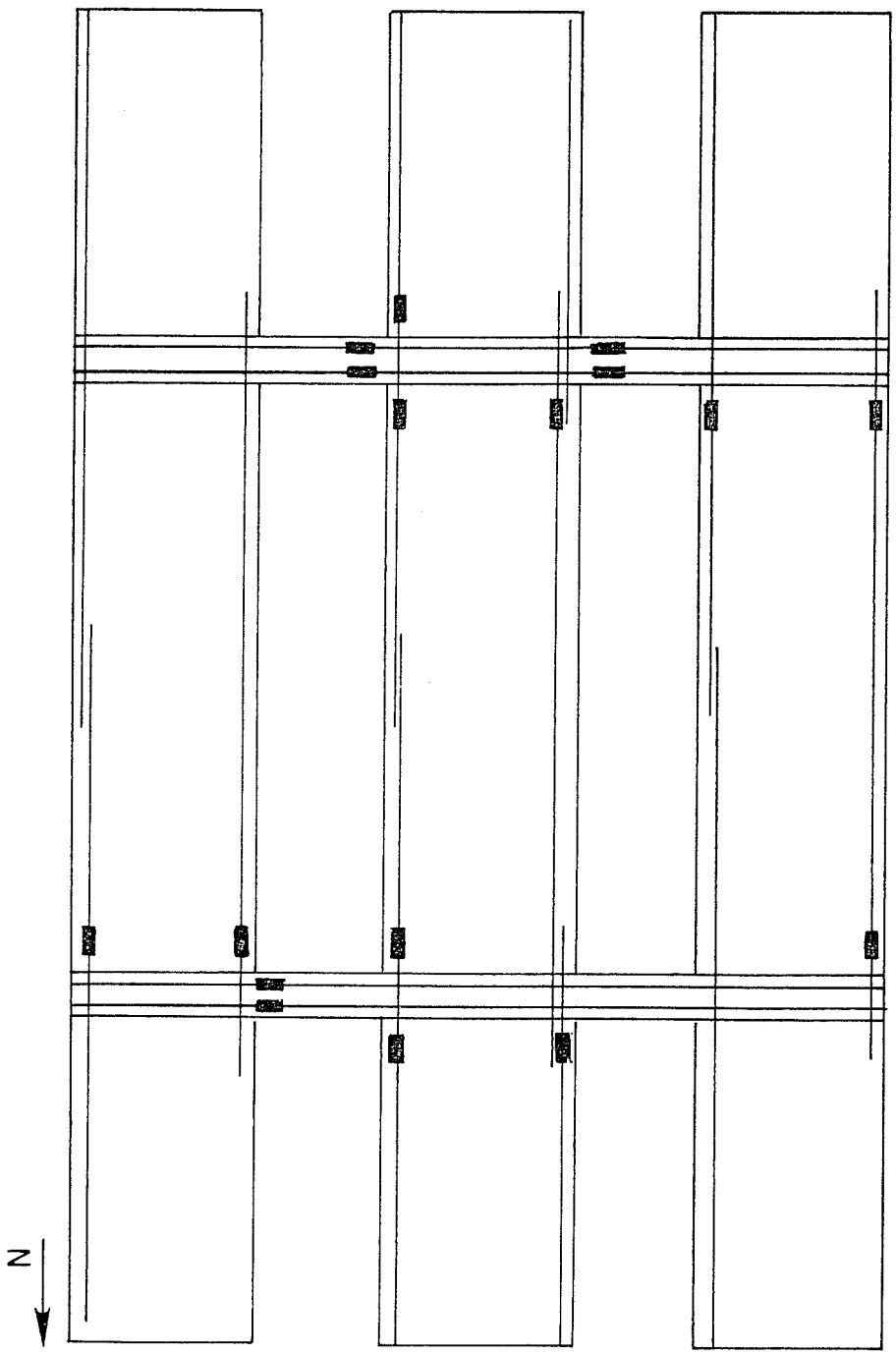


Fig. 3.31 Strain Gages on Steel Reinforcement

# CHAPTER 4

## BEHAVIOR OF SPECIMEN

### 4.1 Load/Displacement History

The specimen was subjected to four series of tests. These included two tests at low load and displacement levels on the bare, or original, frame; a test of the specimen strengthened by concrete wingwalls to displacement levels which produced flexural hinging in the spandrel beams; and a test to failure of the frame strengthened by steel bracing. The general testing procedure and the loads and displacements which were applied to the test specimen are described in this section.

4.1.1 Loading Procedure. In each load series the frame was subjected to reversed cyclic loading, with each cycle beginning in the north direction. Normally the frame was cycled three times at a specified lateral load or drift level before it was subjected to larger displacements. For the first portion of a test, each set of three cycles was kept at the same load level in the north and south directions. In subsequent cycles, the peaks were controlled by imposing equal drifts in the two directions. The drift used to determine the peaks was measured between the first and third floors of the model and will be referred to as total drift.

During testing, an X-Y recorder provided a continuous plot of the applied lateral load versus the third level displacement from the reaction wall. An example of the plots, in Fig. 4.1, shows the last three cycles applied to the steel braced frame.

The strengthened frame tests were carried out over a period of three to four days to permit adequate time for recording data and making visual observations of damage. Data were recorded approximately 300 times (load stages) during the test of the steel braced frame. At each load stage, voltages of 96 channels were scanned, converted to engineering units, stored on a permanent disk, and printed at the test site. Dial gage readings were recorded manually, and new cracks were traced with colored markers (different colors for the two directions) and labeled to indicate load stage at which they occurred.

4.1.2 Previous Tests. The purpose of the two bare frame tests was to determine the initial stiffness of the

unstrengthened frame and to check out the instrumentation and loading system. To do this without damaging the columns, maximum lateral load applied was 32 kips which is less than the nominal shear strength of 62 kips for two columns. Both tests consisted of two cycles to 32 kips in each direction. The total drift between the first and third floors was about 0.06 percent, with the frame slightly less stiff during the second test. At this displacement flexural cracks appeared in the spandrels near the corners of the columns, but there were no column shear cracks.

The displacement levels imposed on the concrete strengthened frame are displayed in Fig. 4.2. Four sets of three cycles were performed at increasing drift levels. The last three cycles were at 0.5 percent total drift, with the interstory drifts approximately equal. At this displacement level, there was extensive cracking of the spandrels with hinging near the piers. Some shear cracks in the piers crossed the original column.

4.1.3 Steel Strengthening Test. Figure 4.3 shows the displacement history of the frame strengthened by steel bracing. To check out the instrumentation, two preliminary cycles were performed at low load levels: one to a peak of 30 kips, the other to 60 kips. The frame was then subjected to two sets of cycles controlled by equal loads in the two directions. The peak loads were 90 and 150 kips which corresponded, respectively, to about 0.1 and 0.17 percent total drifts.

The remaining cycles were controlled by drift levels between the first and third story. For cycles exceeding 150 kips, three cycles at a drift level of 0.23 pecent, three cycles at 0.36 percent, and three cycles at increasing displacement levels up to 0.84 percent drift were applied. The interstory drift between the second and third level was over 1 percent in the final cycles. The differences in interstory drift between the two levels will be discussed in Section 4.3.

## 4.2 Behavior During Test of Steel Braced Frame

Load-displacement curves representing the entire load history are shown in Figs. 4.4 and 4.5. Positive loads and displacements correspond to pushing the frame in the north direction. The two graphs are at different scales. Figure 4.4 displays the first cycles at each load or displacement level except for the final three cycles which are shown in Fig. 4.5. The final three cycles will be referred to as the F1, F2, and F3 cycles. The behavior of the steel-braced frame will be

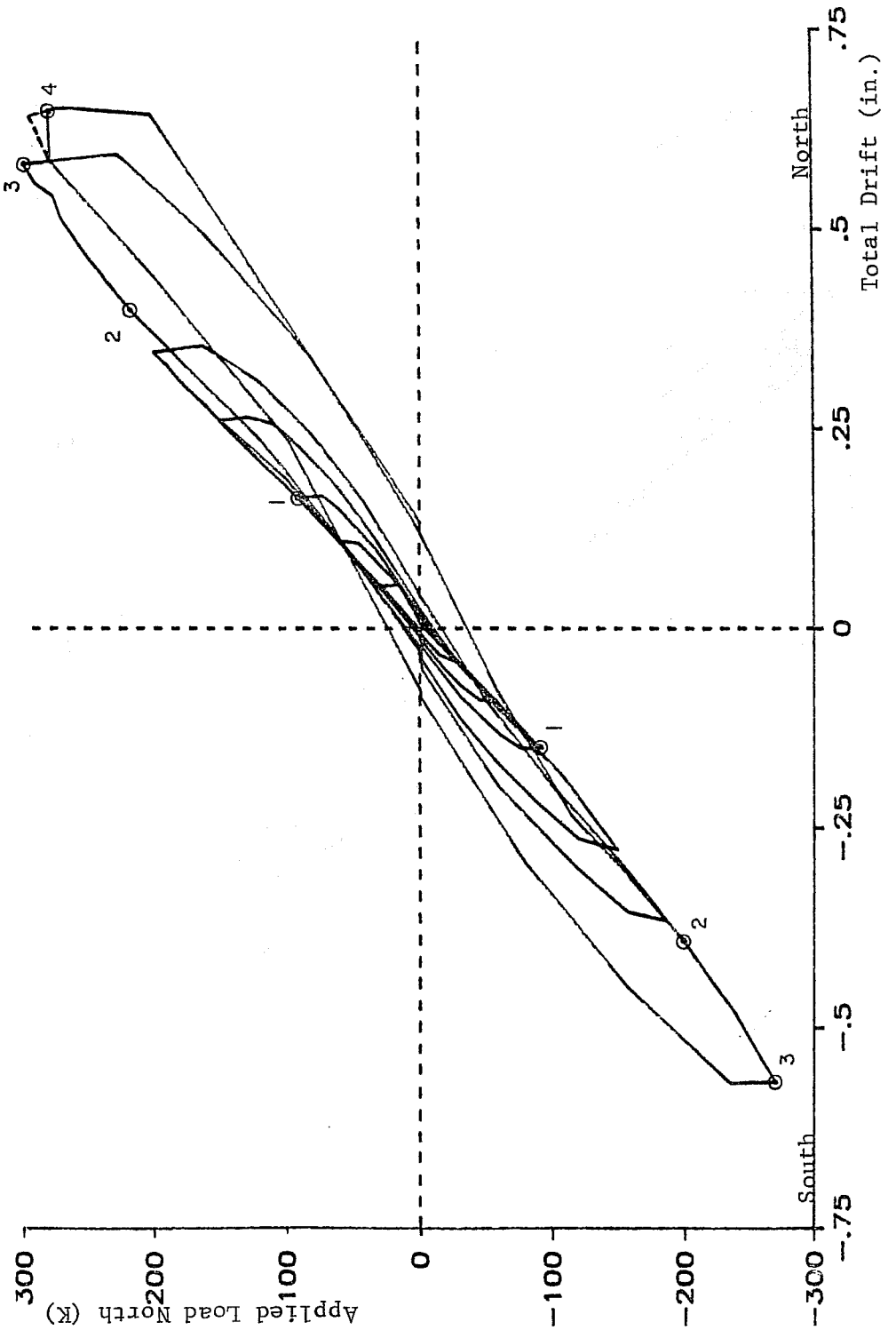


Fig. 4.4 First cycles through 300 kips

described using load-drift reference points circled in Figs. 4.4 and 4.5 and the brace notation in Fig. 4.7.

During the preliminary cycles to 30 and 60 kips, cracks from previous tests began to reopen. The most significant cracks were the shear cracks on the slab side of the columns which had formed during the test of the concrete strengthened frame. New cracks did not appear until a load level of 90 kips and 0.1 percent total drift was reached (points labeled 1 in Fig. 4.4). Figure 4.6(a) shows the crack patterns at point 1 in the north column at the second level.

A total drift of 0.25 percent was attained (points labeled 2 in Fig. 4.4) when 220 kips was applied in the north direction and 200 kips in the south direction. A significant increase in column cracking did not occur until 0.4 percent drift was reached at about 300 kips (points labelled 3). Figure 4.6(b) shows the cracking at the same location as Fig. 4.6(a) but at the higher drift level. The new shear cracks in the columns and flexural cracks in the spandrels can be seen.

After the three cycles at 0.4 percent drift, loading to the next drift level commenced. At a lateral load of 295 kips to the north, a brace weld broke, and the load dropped to 280 kips. In Fig. 4.4, the dotted line represents the increase in load to 295 kips and the sudden drop when the weld failed. This is only an estimate of the load-deflection points since a scan of the instrumentation channels was not made until the load leveled off at 280 kips (point 4). The brace-to-gusset plate welds at the bottom of brace B1 (Fig. 4.7) fractured. Upon examination, it was determined that the weld was defective in that full weld penetration had not been obtained. The frame was unloaded, and the connection was rewelded.

After rewelding, loading was started again in the north direction, as shown in Fig. 4.5. When the load reached 330 kips (point 5), part of the weld at the top of brace T2 broke. The welds connecting the interior flange and part of the web to the gusset plates failed leaving the exterior flange to carry the entire brace load. The weld on the outer flanges was able to transfer the load produced by the brace flange yielding in tension. The load was removed, and the connection was rewelded. Loading continued in the south direction up to 300 kips when the weld connecting the web at the bottom of brace T3 failed, reducing the applied lateral load to 290 kips. Data were recorded at this load (point 6). At this time all welds were inspected. The entire middle connection between braces 2 and 3 was rewelded. Nearly all other brace welds were strengthened to ensure that the

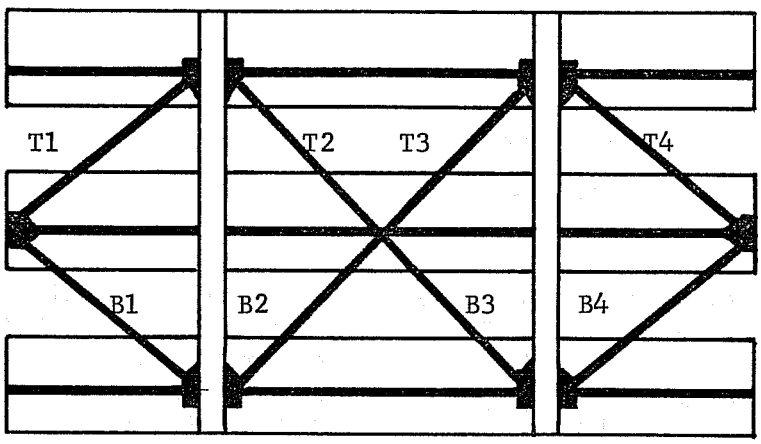


Fig. 4.7 Brace notation

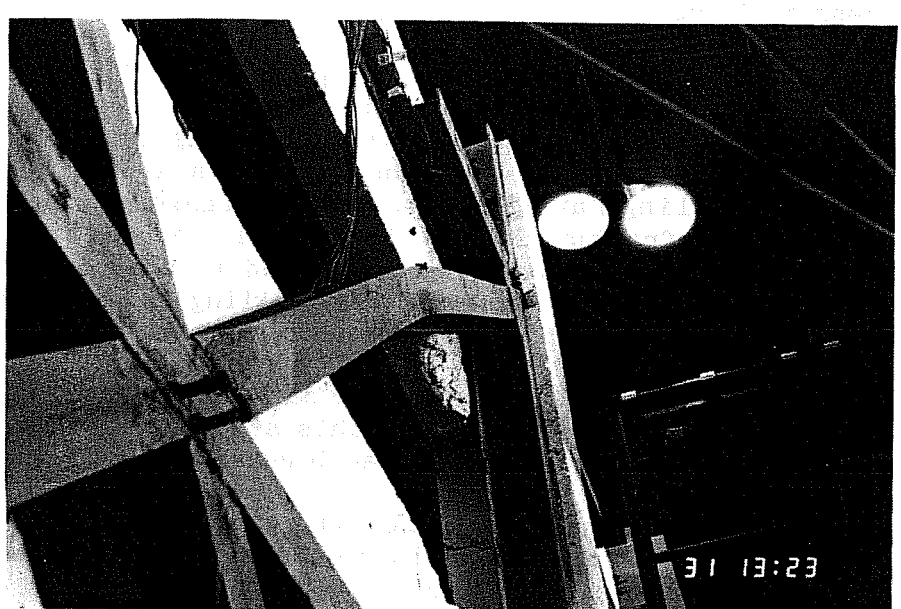


Fig. 4.8 Buckled brace T3

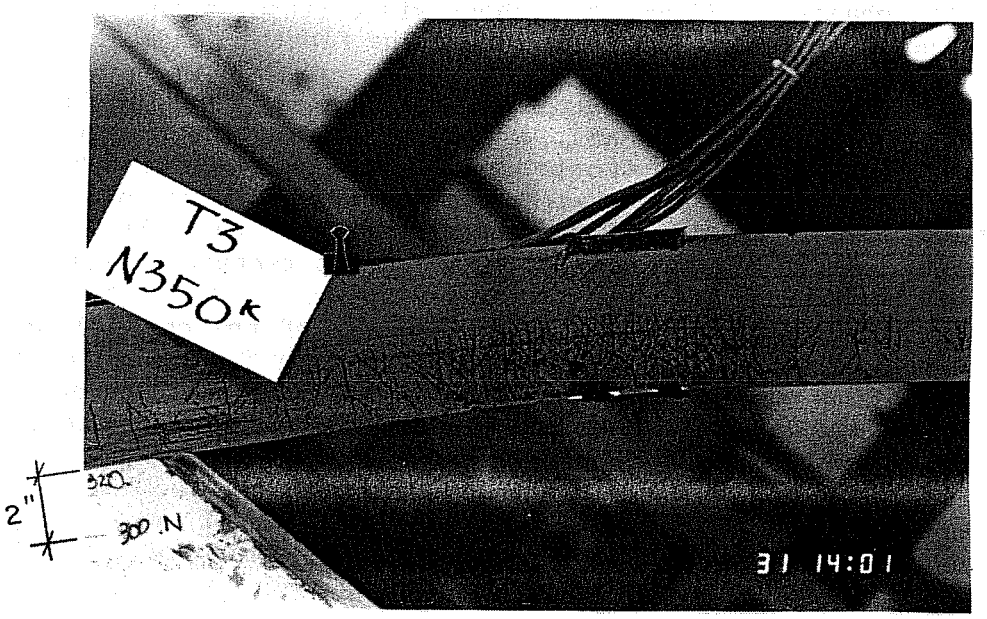


Fig. 4.9 Brace T3 hinge

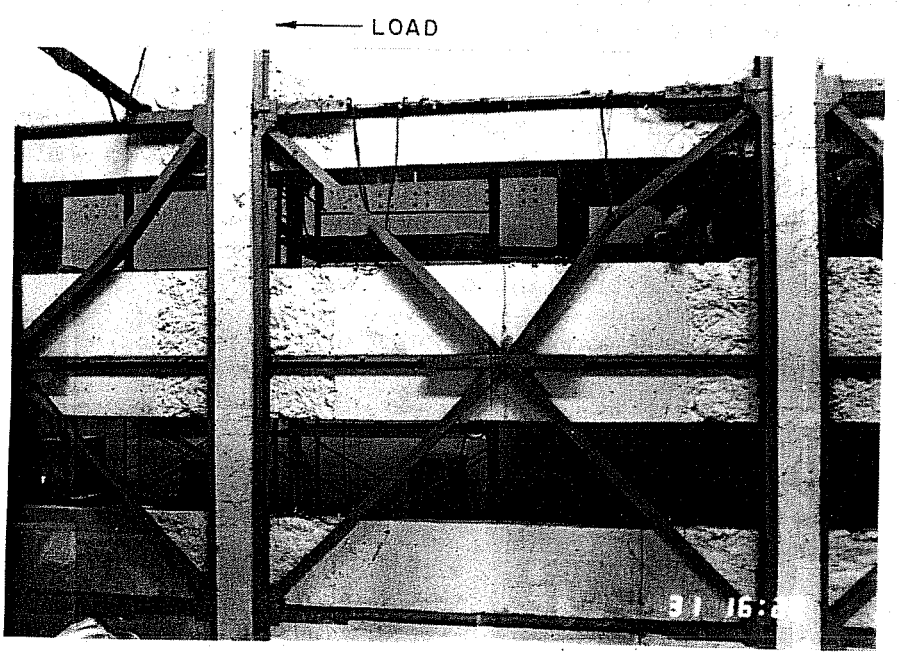


Fig. 4.10 Braces at peak load north

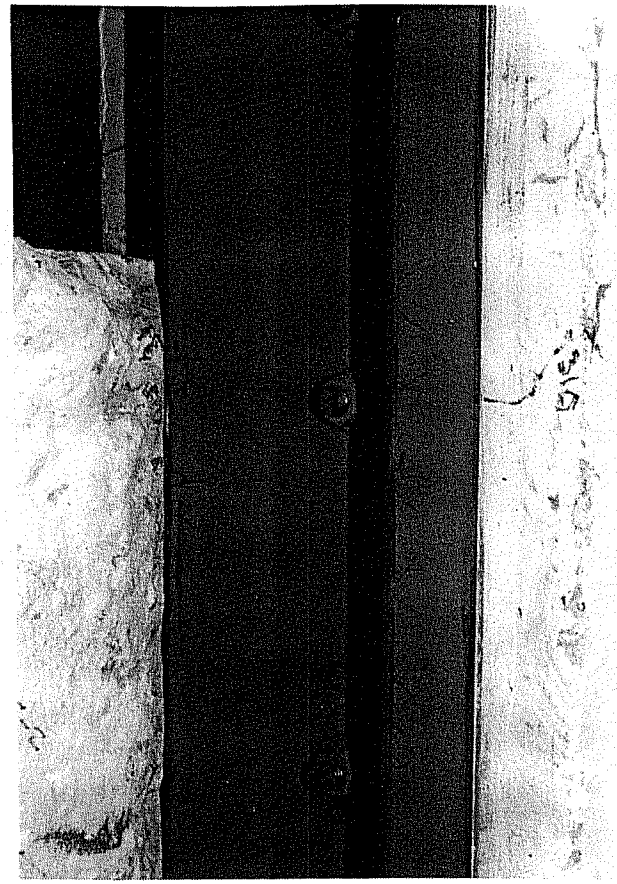

Fig. 4.11 Compression yield lines on channel

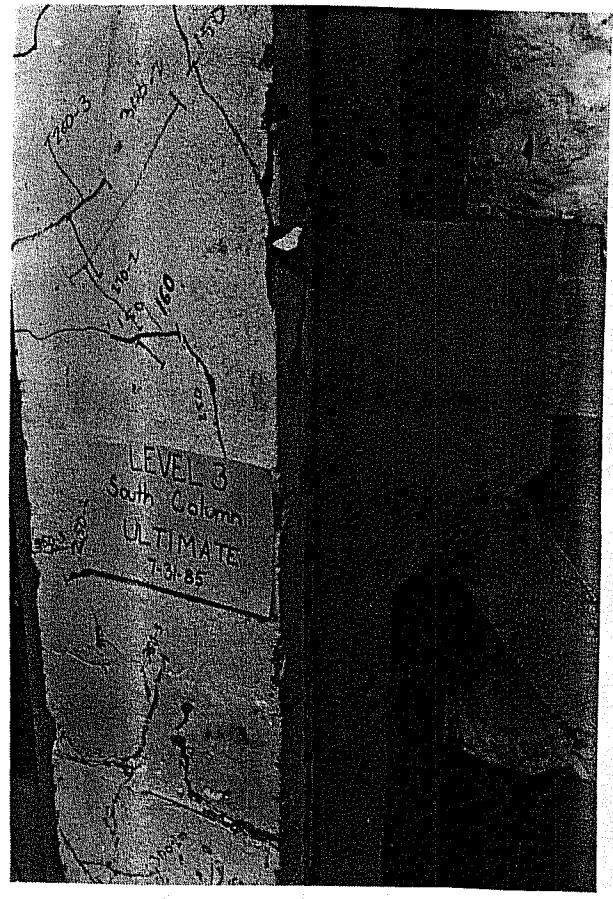


Fig. 4.12 Dowel pullout

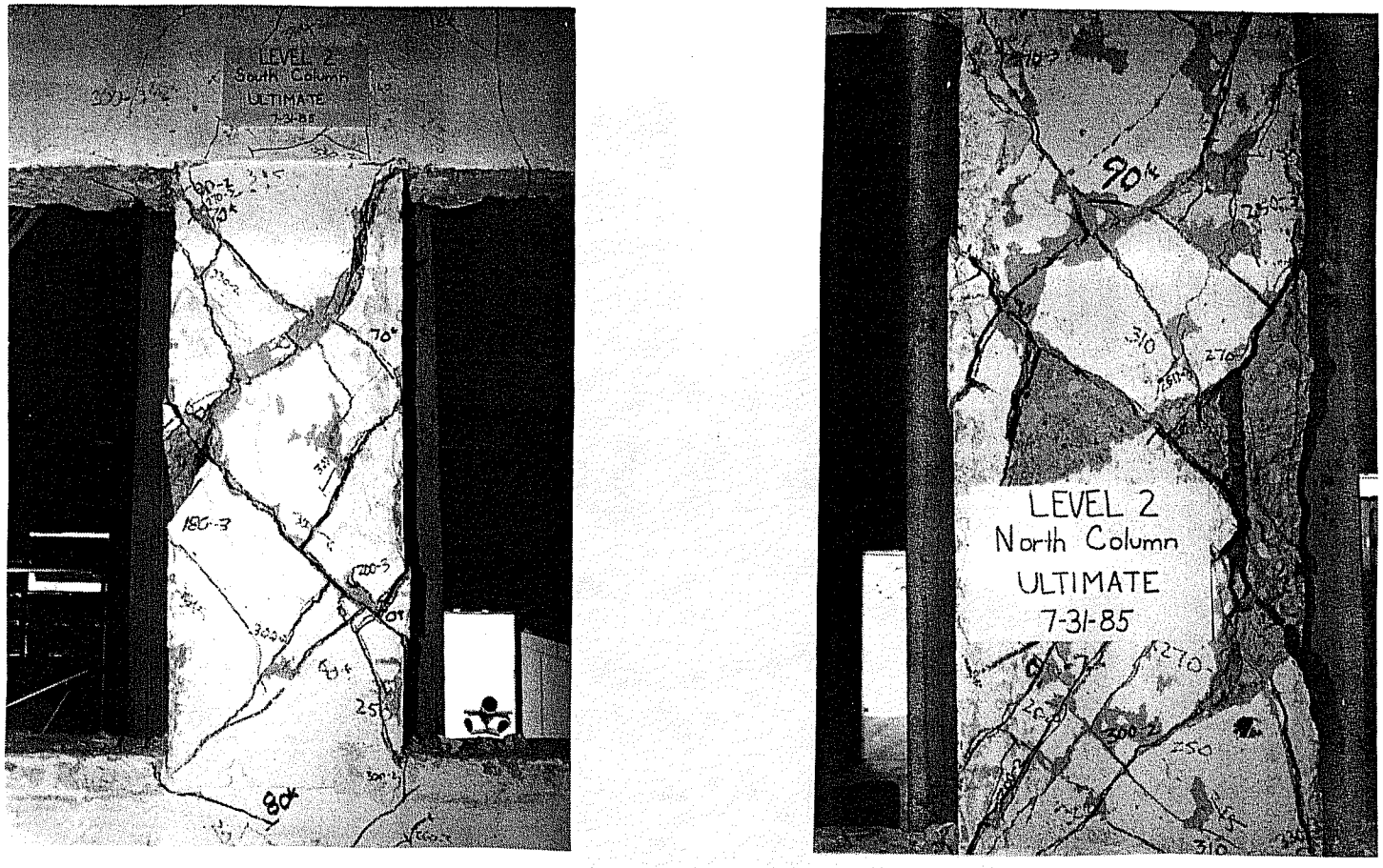


(a) South column

(b) North column

Fig. 4.15 Second level columns at ultimate

assembly. Part of the fracture surface was through the brace flange rather than through the weld or weld-steel interface. Note the diagonal tension yield lines on the brace and the dark region near the end where all the paint had flaked off the surface.

## 4.3 Stiffness of Strengthened Frame

4.3.1 Comparison with Bare Frame. The load-deflection curve for the first of the bare frame tests is shown in Fig. 4.17 along with the first cycle load-deflection curve for the steel braced frame. The curves indicate that the strengthened frame had a stiffness about one and a half times that of the original frame. It must be noted that the steel braced frame was initially cracked which reduced its stiffness.

4.3.2 Calculation of Drifts. Drifts were computed from the displacement transducer data as described in Section 3.4.2.1. Table 4.1 shows the drift levels, in percent, for the single-story and two-story drifts. The values at all peak loads are given, except where they are the same in the second and third cycles. The loads near the end of the test which are not necessarily peak loads (because the load dropped before the data could be obtained) are shown in parentheses.

The interstory drifts were about equal at the start, but at load levels exceeding 200 kips there were differences between the drifts in the two directions. In the north direction, the first level was more flexible, while in the south direction, the second level showed less stiffness. As the test progressed, the second level became less and less stiff when the frame was pushed south. In the north direction, the second level did not become the more flexible story until cycle F2, which was when the first brace buckled.

The difference in interstory drifts is obvious from Fig. 4.18 where load-drift curves are compared for the last set of cycles. A maximum drift of about 1 in. occurred in the second story, whereas the largest value for the first level was 0.43 inches. Even without the last cycle (where failure in the second level occurred) the second level drifts were larger than the first, especially in the south direction. Unless otherwise stated, the drift values presented refer to the total two-story drifts.

Table 4.1 Drifts at Peaks - Steel Test

| Load North (kips) | % Drift First Level | % Drift Second Level | % Drift Total |
|---|---|---|---|
| 91 | 0.105 | 0.100 | 0.102 |
| 150 | 0.174 | 0.152 | 0.163 |
| 200 | 0.228 | 0.206 | 0.217 |
| 211 | 0.248 | 0.217 | 0.232 |
| 199 | 0.239 | 0.220 | 0.230 |
| 300 | 0.380 | 0.347 | 0.363 |
| 298 | 0.394 | 0.334 | 0.364 |
| 286 | 0.383 | 0.351 | 0.367 |
| 331 | 0.476 | 0.436 | 0.456 |
| 352 | 0.517 | 0.586 | 0.551 |
| 357 | 0.544 | 0.680 | 0.612 |
| (316) | 0.528 | 0.773 | 0.650 |
| (237) | 0.492 | 1.182 | 0.837 |
| **Load South (kips)** | | | |
| 91 | 0.086 | 0.103 | 0.094 |
| 150 | 0.149 | 0.198 | 0.173 |
| 185 | 0.205 | 0.252 | 0.228 |
| 180 | 0.204 | 0.254 | 0.229 |
| 270 | 0.312 | 0.398 | 0.355 |
| 264 | 0.310 | 0.400 | 0.355 |
| 257 | 0.308 | 0.401 | 0.354 |
| (289) | 0.342 | 0.503 | 0.423 |
| 309 | 0.396 | 0.613 | 0.504 |
| (215) | 0.296 | 0.735 | 0.516 |
| (125) | 0.247 | 1.308 | 0.778 |

4.3.3 Loss of Stiffness. Figure 4.19 is a graph of the first cycles up to a load level of 200 kips. There was no apparent loss of stiffness at this stage. However, the two directions seemed to be behaving differently. Drawing secant stiffness lines to each peak in the north direction would indicate a slight increase in stiffness between 60 and 200 kips. Doing the same in the south direction shows a decrease in stiffness between peaks. The increase in stiffness in the north direction may have been caused by friction between the loading frame and the concrete specimen. When loaded north, the spandrel at the third level came in contact with the end plate on the two structural tubes of the loading frame. The spandrel and the plate moved apart when the frame was pushed south.

At these displacement levels, there was essentially no loss in stiffness during the second and third cycles of a set, as verified by Fig. 4.20. This graph shows all three cycles of the set at 0.23 percent drift. There were only slight decreases in stiffness in the north direction with each cycle.

In subsequent cycles, the loss in stiffness is more apparent. In Fig. 4.21, the three cycles at 0.36 percent drift are overlain with a load-displacement envelope of all previous cycles. Both directions indicate a reduction in stiffness between 200 and 300 kips, and small losses with each new cycle.

The decrease in stiffness was continued into the last set of cycles, as shown in Fig. 4.22. The envelope of previous loads is drawn with the final three cycles. In the north direction, there was a loss in stiffness with each new cycle. In the south direction, the stiffness remained the same for the first cycle, but the frame became more flexible with each of the two remaining cycles. The dramatic loss in stiffness for both directions occurred when the welds failed on the tension braces.

## 4.4 Discussion of Connections

The connections of the steel bracing system, welded steel-to-steel and dowelled steel-to-concrete connections, had a major effect on the behavior of the frame with respect to lateral capacity, stiffness, and ductility. Specifically, improvements in the design and quality control of the welded brace-to-gusset plate connections and the layout of dowels in the column channels would have transferred the failure mechanism from the connections to the steel members and, thus, would have produced more ductile

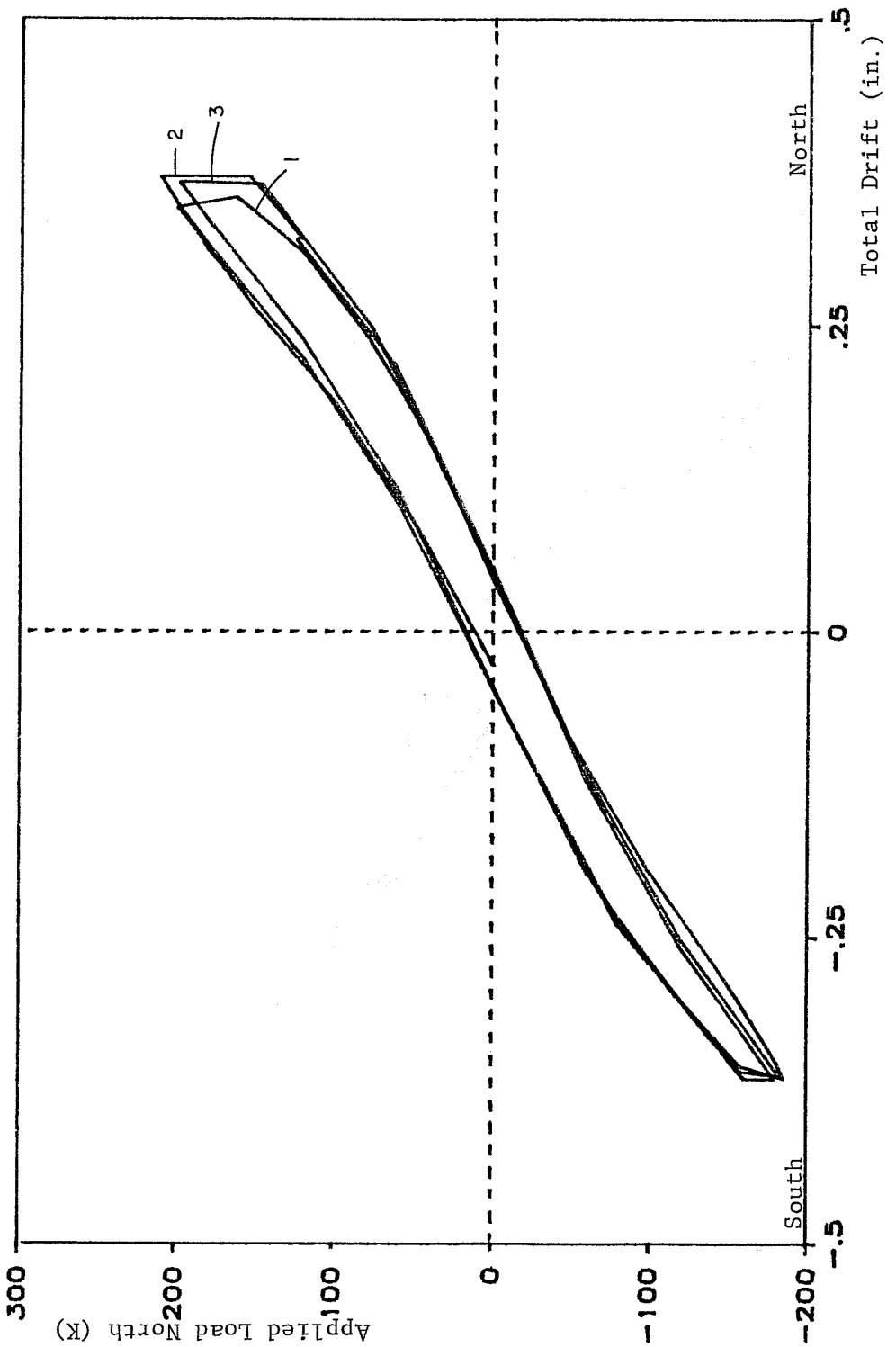


Fig. 4.20 Set of three cycles at 0.23% drift

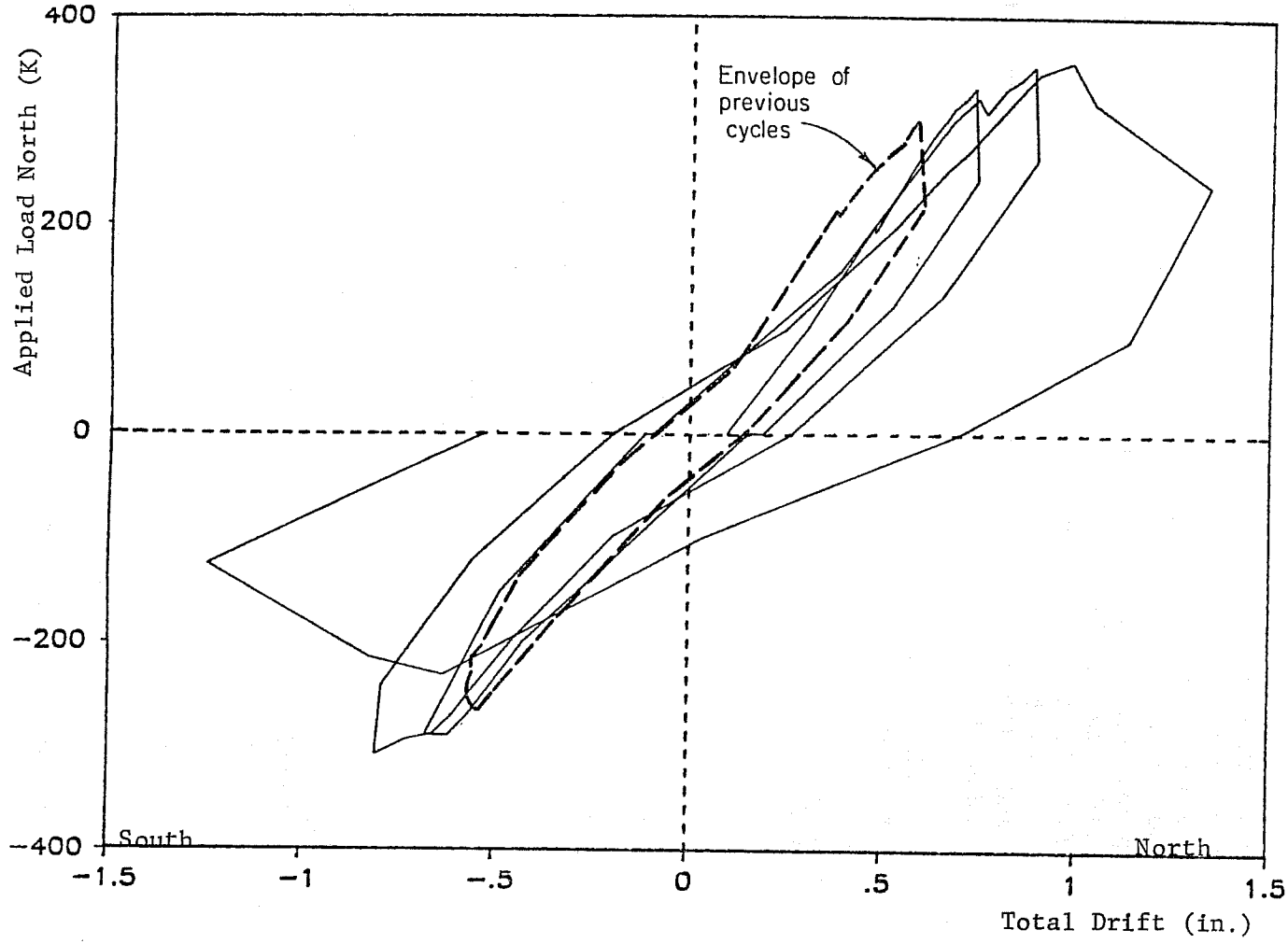


Fig. 4.22 Load-displacement relationships for entire test

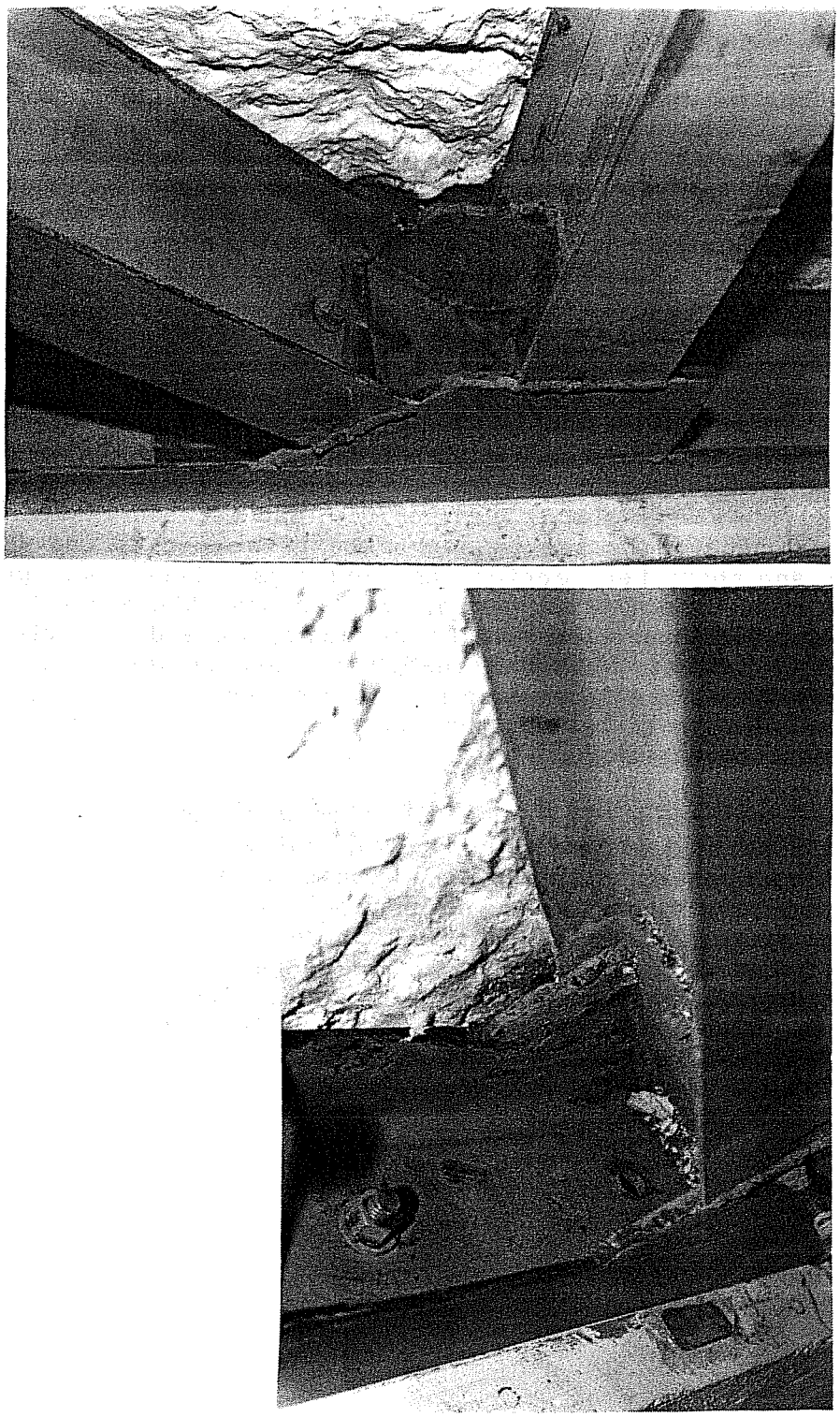

Fig. 4.23 Close-up of welded connection

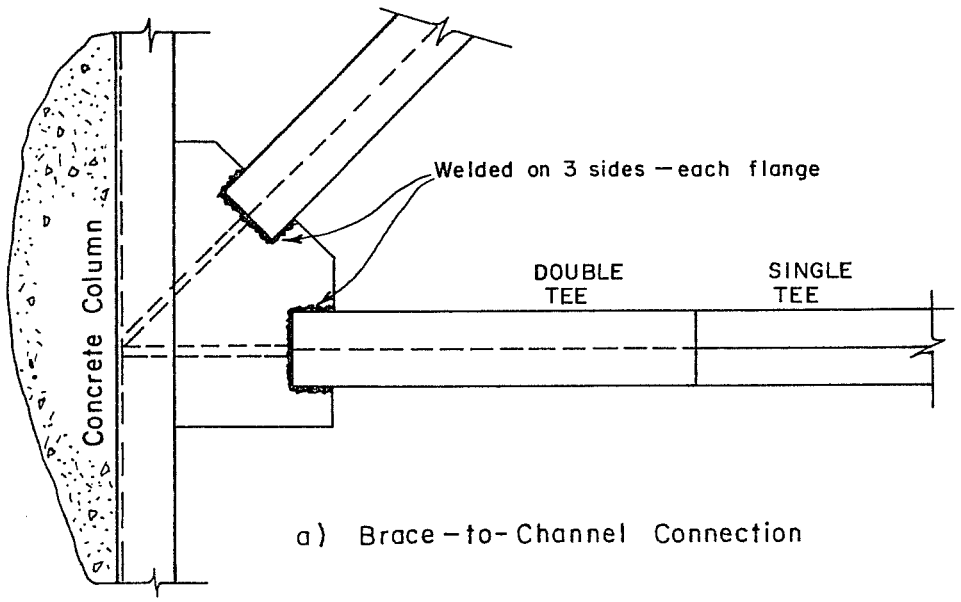


a) Brace-to-Channel Connection

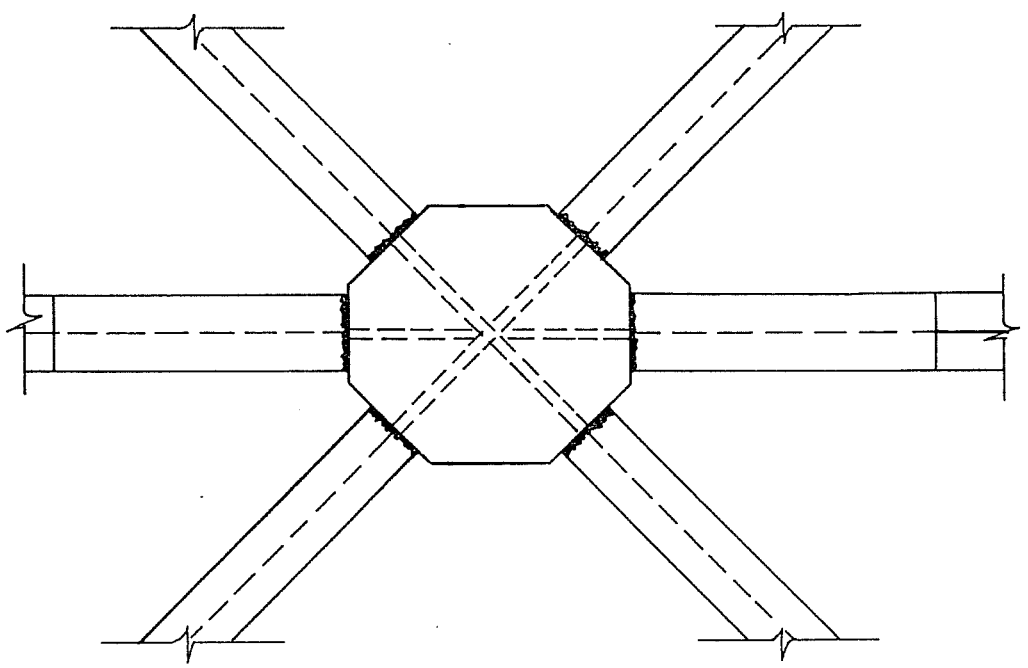

b) Middle Connection

Fig. 4.24 Alternate Connection Designs

# CHAPTER 5

## DETAILS OF TEST RESULTS

### 5.1 Behavior of Braces

5.1.1 Strains. Strain gages were attached to six of the diagonal braces in groups of four as was shown in Figs. 3.27 and 3.28. The gages were placed on the inner side of the flanges close to the tips where maximum bending stresses were expected to occur.

The strains measured using each set of four gages were plotted to determine the consistency of readings at a section. Figure 5.1 displays the strains from the four gages on brace B3 for all load cycles on the steel braced frame (brace notation - Fig. 4.7). The four strains were consistent except for the strain measured by gage number 22 during the three cycles to peak lateral loads of 90 kips. Before loading further the bad gage was replaced, and the four strains were consistent for the remainder of the test. The axial force in brace B3 was computed using the four strains for all load stages except those during the three cycles to 90 kips lateral load where the strains from the three good gages were used.

Strains measured in the other braces were very similar to the strains plotted in Fig. 5.1. Two gages on braces at the upper level had to be replaced during the test after inconsistent strains were recorded during the early cycles. In all subsequent cycles, brace axial load was calculated using the average of the four strains.

The arrangement of strain gages on the four flange tips at the mid-length of the brace was chosen so that the initiation of buckling could easily be monitored. Figures 5.2 and 5.3 display the onset of instability in braces T2 and T3.

The strains in brace T2 plotted versus applied lateral load are shown in Fig. 5.2(a) for the portion of cycle F1 (first of the final three cycles - Fig. 4.5) when the frame was pushed south. At 200 kips lateral load, strains at two locations (flanges on same side of web) leveled off while strains at the opposite side began to increase at a faster rate. After 270 kips lateral load, strains in two gages started dropping due to bending of the brace. After reaching the peak load in cycle F1 (290 kips), the frame was unloaded. The strains observed when the frame was loaded south in the next cycle are shown in Fig.

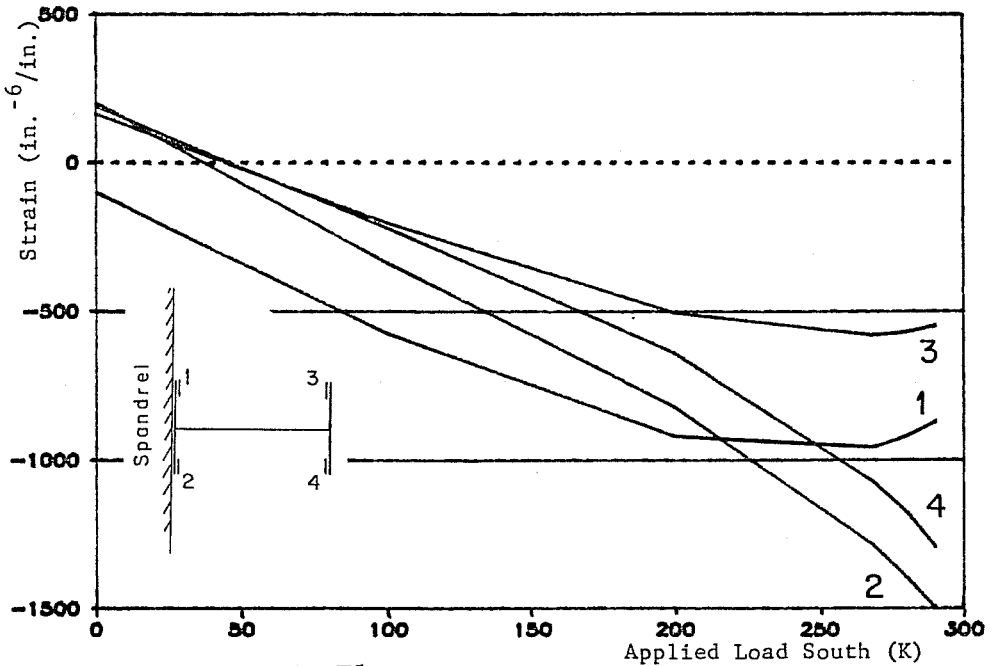


a) Cycle F1

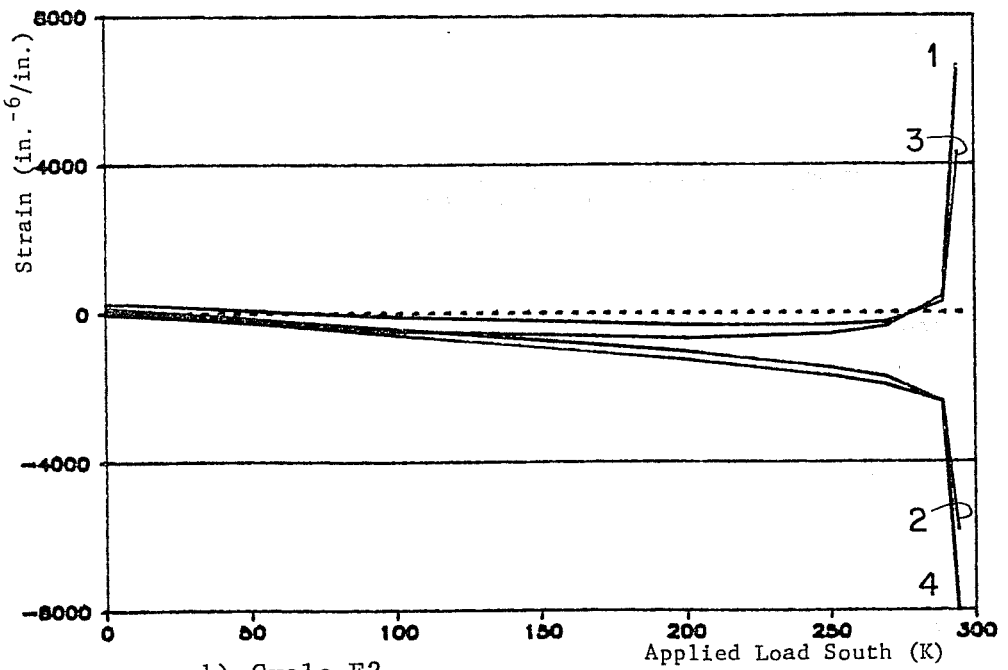


b) Cycle F2

Fig. 5.2 Buckling of Brace T2

5.2(b), which has a different scale than Fig. 5.2(a). The brace buckled before the peak lateral load of 309 kips was reached. At lateral loads in excess of 290 kips, strains were very large indicating general yielding at that location. Observations of the brace clearly indicated that a hinge had formed at the mid-length of the brace.

In Fig. 5.3(a) brace T3 was beginning to show some bending at the north peak of cycle F1 (first of the three final cycles). The graph in Fig. 5.3(b), which is at a different scale than Fig. 5.3(a), shows that the strains began to deviate at an applied load of only 160 kips during cycle F2. At 321 kips, under constant displacement of the frame, brace T3 buckled and the lateral load dropped to 306 kips. The graph is terminated at this level because the gages were no longer reliable.

An example of a complete cycle of a set of four strain readings is shown in Fig. 5.4 for brace T4 during the second of the final three cycles. At the peak lateral load to the south, the brace became unstable, but deformation was not so large that the gages were lost. The arrows show that strain increased at two gages and decreased at the other two during the increase in lateral load to the south from 294 to 309 kips. After this level, the readings from the four gages may not be useful in computing the axial load in the brace due to the localized yielding at the mid-length of the member.

5.1.2 Brace Loads. For all six instrumented braces, the average strain was computed, and from that the average stress, axial load, and horizontal component of the axial load were calculated. The loads were reliable for load stages before brace instability was reached; the axial load carried by a brace could not be determined after buckling.

5.1.2.1 Comparison of Brace Loads. Figures 5.5 to 5.7 display the redistribution of loads between the top four braces. In each graph, the horizontal component of the axial load in the brace is plotted against the applied lateral load. In Fig. 5.5, the loading from zero to 290 kips south during cycle F1 is shown. A scan was taken at 290 kips, just before part of the T3 weld broke and the load dropped to 289 kips where another scan was taken. The horizontal load carried by brace T3 dropped 23 kips while the loads in braces T1, T2 and T4, respectively, increased by 3, 3, and 7 kips. This left 9 kips unaccounted for which may have been carried as shear in the columns.

The portion of cycle F2 is shown in Fig. 5.6 for loading from zero to 356 kips north. When the applied load reached 321 kips, the displacement was held constant while brace T3 buckled

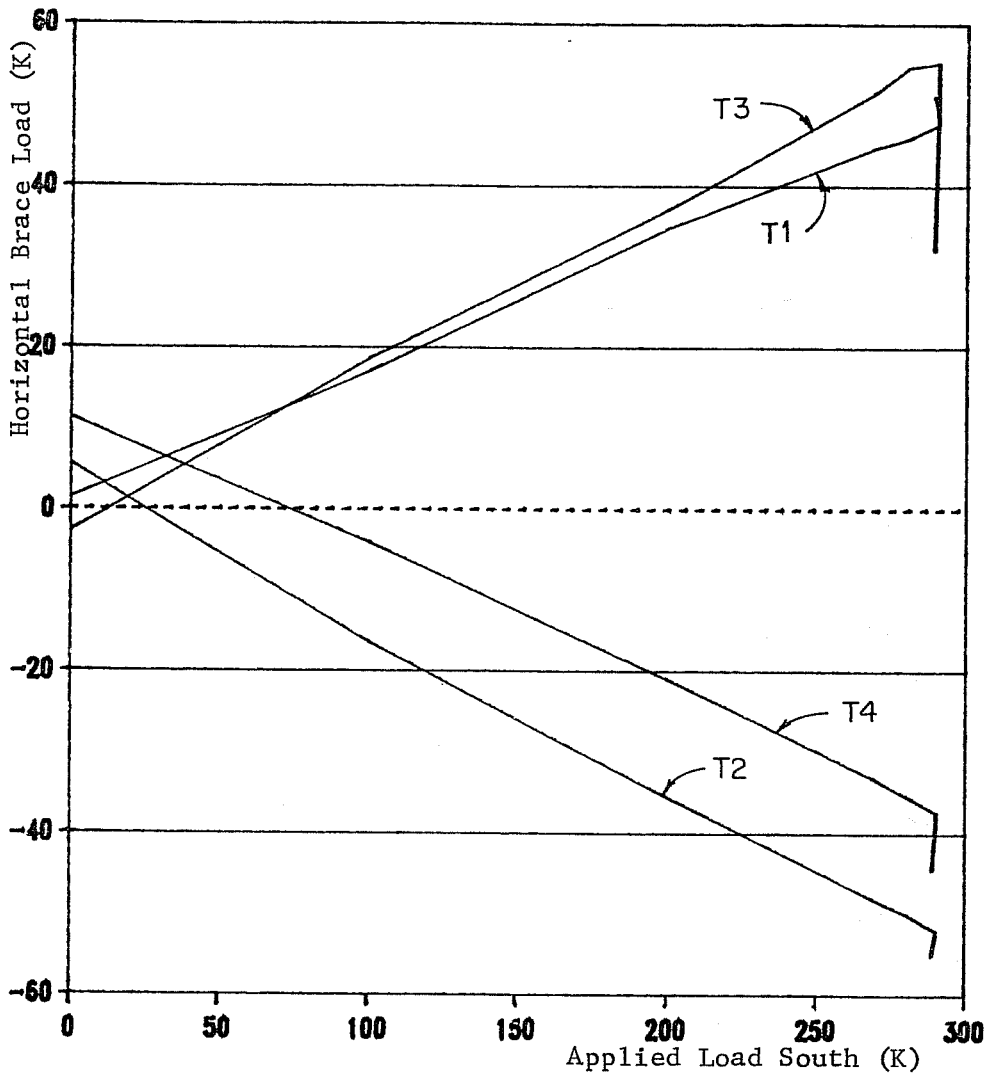


Fig. 5.5 Brace Loads During F1 Cycle - South

and the load dropped to 306 kips. During this step, the horizontal load carried by brace T1 increased by 2 kips, brace T2 stayed the same, and brace T4 picked up 2 kips. The load in brace T3 is plotted, but after about 290 kips the loads are not reliable. Between 321 and 356 kips, brace T4 picked up load at a higher rate than it had before brace T3 buckled, but the slopes for T1 and T2 remained approximately the same.

Figure 5.7 shows the stage at which brace T2 buckled during the F2 cycle south. The axial load in brace T3 is not plotted because it had buckled during the previous load north, and the gages were unreliable. After a lateral load of 290 kips was attained, braces T1 and T4 began picking up axial load at a faster rate, and it is unclear what load brace T2 was carrying.

The loads in the braces were plotted versus the applied load to compare the axial loads in each of the top level braces during the entire test. The loads at the peak of each cycle were plotted as shown in Fig. 5.8. The peaks in the north and south directions were plotted on separate graphs through the second of the final three cycles.

Residual strains increased during cyclic loading. To produce a plot of the increment in axial force versus the increment in applied lateral load, the peak brace loads were adjusted by subtracting the axial force at the previous point of zero applied load. The increment in axial load from zero applied load will be referred to as "adjusted" brace load.

In general, the two graphs indicate that the middle braces (T2, T3) carried higher loads than the outer braces (T1, T4) until the end of the test when the middle braces had buckled. In compression, the middle braces carried about 25 percent more load, while in tension they had about 15 percent more load than the outer braces. In the last load stage shown in the north direction (350 kips), brace T3 had buckled and is not displayed since the load could not be determined. The axial loads in T1, T2 and T4 jumped up at this stage. In the graph for south load peaks, braces T2 and T3 had previously buckled so are not shown in the last load stage (309 kips). The loads in both T1 and T4 showed a large increase between 290 and 309 kips lateral load. the line in the second graph of Fig. 5.8 marks the stage when part of the weld in brace T3 failed. The load in T3 dropped while the other three brace loads increased.

The brace loads were also compared by plotting them versus the interstory drift. This was done due to the differences in drift in the two directions and between the two

stories at a given load. The four middle braces (T2, T3, B2, and B3) are compared in this manner.

Figure 5.9 shows the axial brace load plotted versus the total drift. Although the two interstory drifts were not equal, the graph allows comparisons of the four brace loads at given total drift levels. The pairs of braces (B2-T3, B3-T2), which are continuous across the connection at the second floor level, followed each other closely until the top level braces buckled. In tension the bottom two continued increasing linearly while in compression they tended to increase very little. The vertical line on the graph marks the stage just after the weld on the web of brace T3 failed.

In Fig. 5.10 the same axial loads are plotted but relative to interstory drift. Thus, the B2 and B3 points are plotted versus first story drift, and the top braces are plotted versus second story drift. The load versus drift points for the top and bottom braces were linear initially. At drifts greater than 0.25 inches, differences may be seen between Figs. 5.9 and 5.10. During the cycles when the top compression brace was bending, the axial load in the bottom compression brace was no longer increasing, and when the top brace buckled, the bottom brace load dropped although the drift level was larger. Even though the bottom compression brace was capable of carrying more load, no load was applied to it since the bottom braces are connected to those above at the X-connection at the second floor level.

5.1.2.2 Discussion of Buckling Loads. Buckling loads were predicted using AISC equation (1.5.1) for inelastic buckling without a safety factor [23].

$$P_{cr} = \left[ 1 - \frac{(KL/r)^2}{2C_c^2} \right] A \times F_y$$

$$\text{where } C_c = \sqrt{2\pi^2 E/F_y}$$

The flange yield strength ($F_y$) of 44.5 ksi obtained from tension tests was inserted in the above equations to compute buckling loads for two different K values. Rows 1 and 2 of Table 5.1 show the predicted buckling loads using the theoretical K-factor of 0.5 and the suggested design value of 0.65. The outside braces, T1 and T4, were shorter than the middle braces resulting in higher loads.

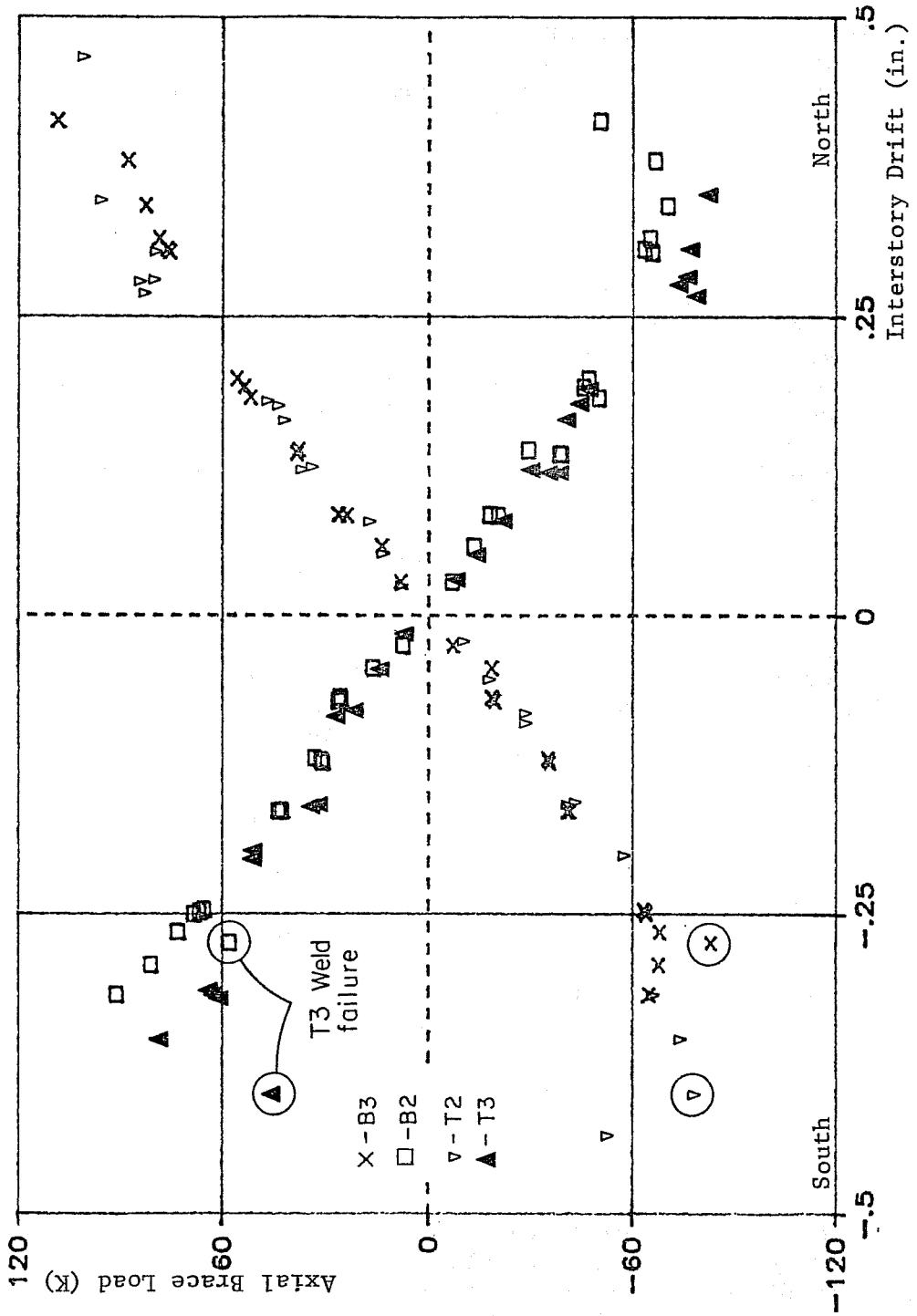


Fig. 5.10 Middle brace loads versus interstory drift

TABLE 5.1 Maximum Loads in Top Braces

| (kips) | T1 | T2 | T3 | T4 |
|---|---|---|---|---|
| Predicted Buckling Load (K = 0.65) | 82 | 79 | 79 | 82 |
| Predicted Buckling Load (K = 0.5) | 93 | 91 | 91 | 93 |
| Maximum Compression Load | 107 | 79 | 83 | 96 |
| Predicted Tension Yield Load | 112 | 112 | 112 | 112 |
| Max. Tension Load | | | | |
| Cycle F1 | 73 | 97 | 79 | 86 |
| Cycle F2 | 87 | 101 | -- | 108 |

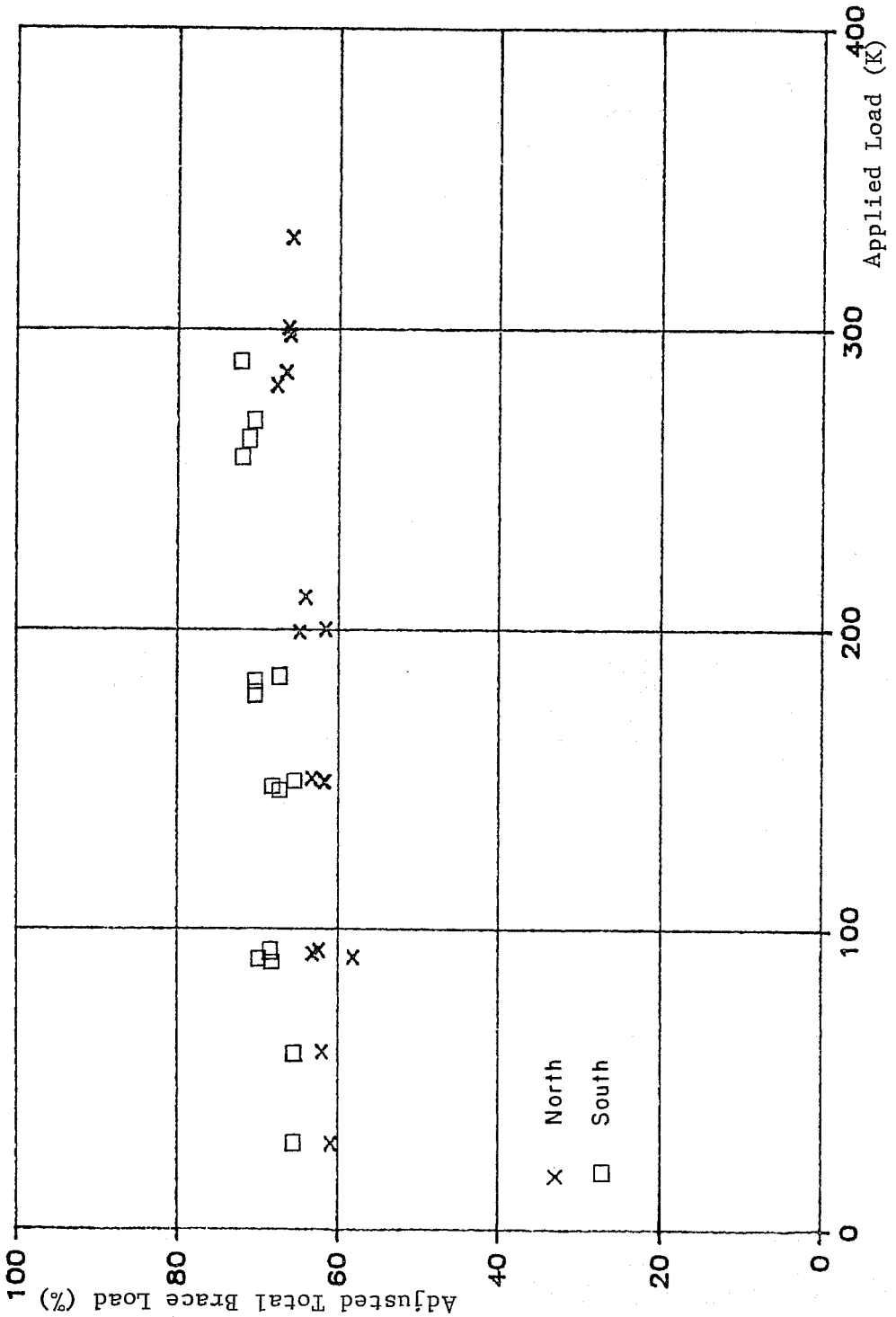


Fig. 5.12 Percent of load carried by braces

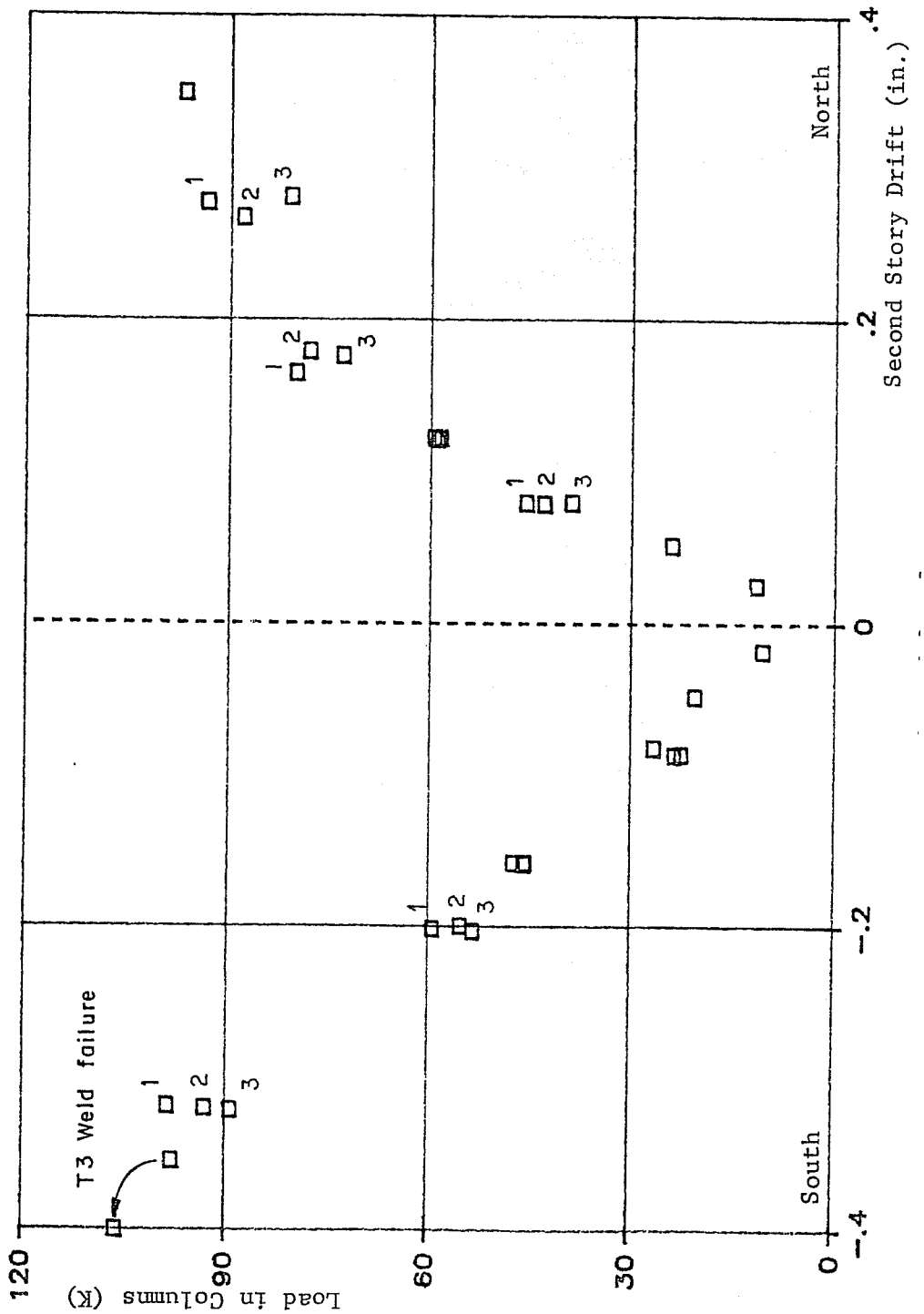


Fig. 5.13 Shear in columns at second level

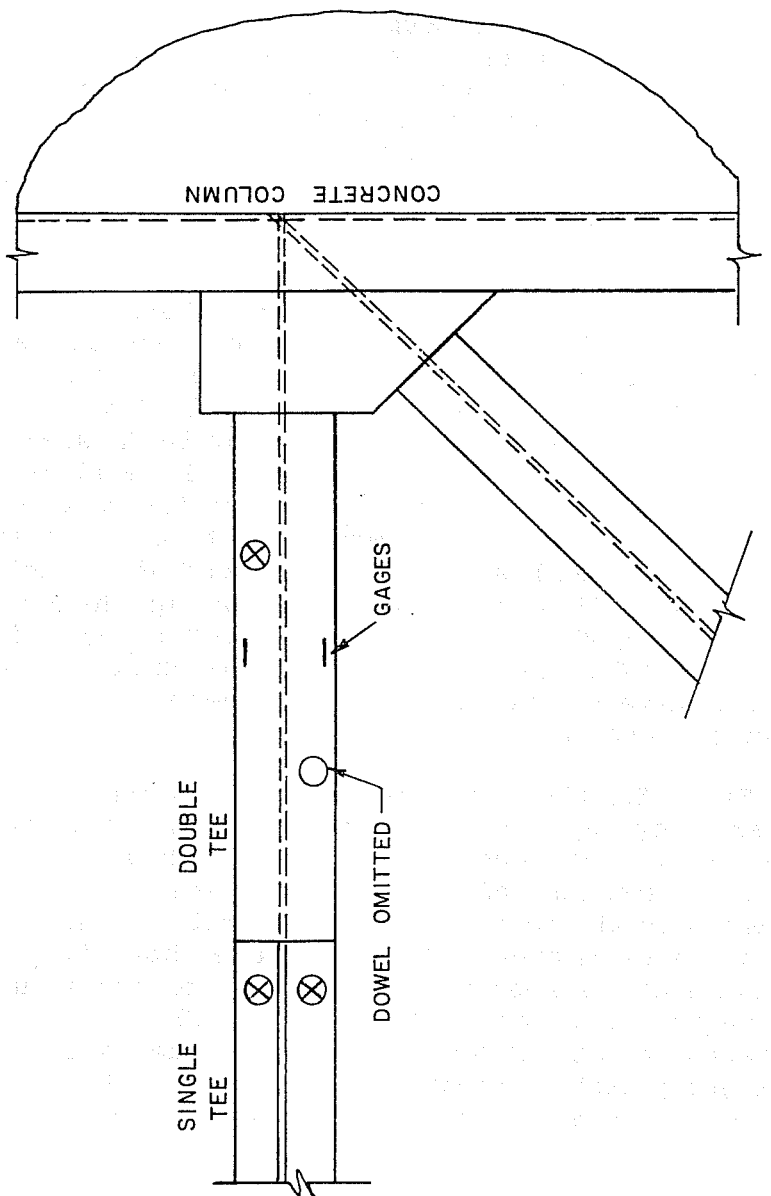


Fig. 5.15 Connection Region at End of Collector

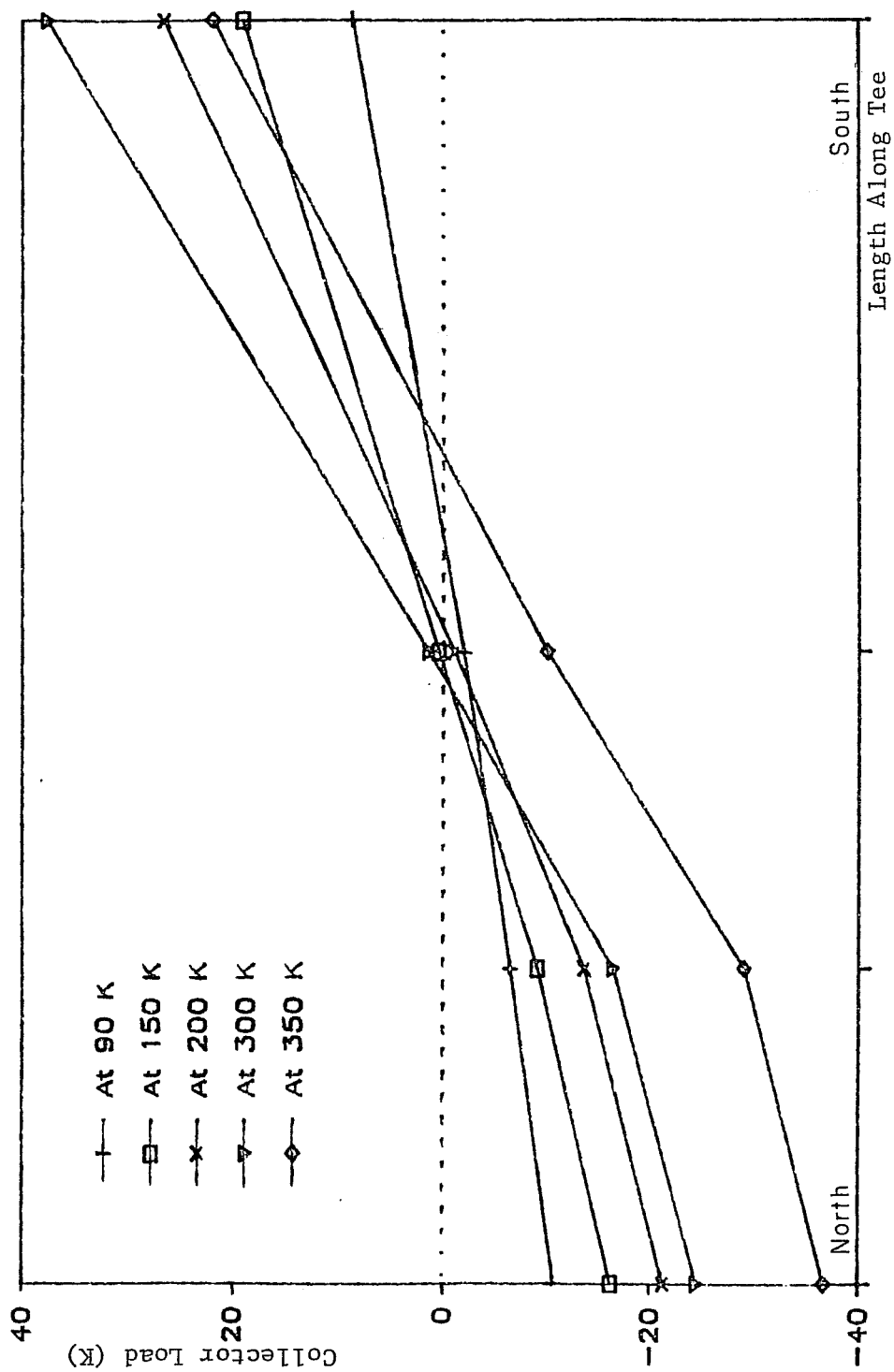


Fig. 5.16 Forces in collector tee at peaks - north load

TABLE 5.2 Forces in Collector Tees (kips)

| Applied Load | Tee-North End | | | Tee-South End | | |
|---|---|---|---|---|---|---|
| | Measured* | Computed** | Meas./Comp. | Measured* | Computed** | Meas./Comp. |
| North | | | | | | |
| 30 | -3.7 | -5.8 | 0.64 | 3.1 | 4.9 | 0.63 |
| 60 | -6.9 | -10.4 | 0.66 | 6.4 | 9.9 | 0.65 |
| 90 | -10.7 | -12.0 | 0.89 | 8.7 | 16.6 | 0.52 |
| 150 | -16.2 | -26.0 | 0.62 | 19 | 21.4 | 0.89 |
| 200 | -21.3 | -29.6 | 0.72 | 26.5 | 29.1 | 0.91 |
| 300 | -24.5 | -59.2 | 0.41 | 37.6 | 52.7 | 0.71 |
| 330 | -27.5 | -67.4 | 0.41 | 39.4 | 58.2 | 0.68 |
| 352 | -36.7 | -70.7 | 0.52 | 21.9 | (T3 buckled) | -- |
| South | | | | | | |
| 30 | 3.9 | 5.6 | 0.70 | -3 | -5.6 | 0.54 |
| 60 | 7 | 12.1 | 0.58 | -6.8 | -10.1 | 0.68 |
| 90 | 10.1 | 22.8 | 0.44 | -11.2 | -14.9 | 0.75 |
| 150 | 19.7 | 29.0 | 0.68 | -16.6 | -31.8 | 0.52 |
| 185 | 24.1 | 40.0 | 0.60 | -21.3 | -35.1 | 0.61 |
| 270 | 32 | 46.1 | 0.69 | -25.8 | -43.7 | 0.59 |
| 290 | 32.2 | 52.0 | 0.62 | -29.8 | -55.2 | 0.54 |

*Measured using strain readings

**Computed from equilibrium of forces at connection, ignoring direct transfer to concrete through connection

difference between web and flange strains was not quite as exaggerated.

Because the cross-section was not symmetric, and the strains were not distributed evenly, a method was devised to compute the channel load which did not take the average of the four strains. The strain distribution which was used assumed that the entire web area had a strain equal to the average of the two web strains and the flanges had a linearly varying strain which was the average web strain at the corner and the flange strain at the tip. Calculation of loads in the above manner produced loads smaller than those computed from the average, as indicated in Table 5.3.

Also shown in Table 5.3 is a comparison of the channel loads and the vertical components of the load in brace B2. Loads were calculated for the instrumented section on the channel closest to where brace B2 frames in to the channel. There was one dowel between the gages and the connection. Ratios of the channel load over the load computed from brace B2 (Avg/Comp and Dist/Comp) are listed in the last columns of the table. When the frame was loaded south and the channel was in compression, the ratio was much smaller than when the frame was pushed north. This may have been caused by differences in the relative positions of the dowels in the holes and by friction between the channel and the column when the brace was in tension.

## 5.3 Relative Displacement

Relative displacement, or slip, between the steel members and the concrete frame were measured in eight locations as shown in Fig. 3.27. Except for the results from the two displacement transducers at the middle connection, the load-slip curves for each location had the same general shape and showed a large increase in slip at loads greater than 200 kips. Some of the transducers became inoperable during the final cycle, so comparison of maximum slips will be made for cycle F2.

Figures 5.19 and 5.20 are load-slip curves for the second half of the test, which began with the three cycles to 0.23 percent drift or 210 kips north and 185 kips south. In both graphs, there is a huge increase in slip after the three cycles to 200 kips, especially when the frame was loaded north. The two locations represented by these graphs are both on the third-level collector tee. However, the slip at the middle connection also showed a large increase after 200 kips lateral load (Fig. 5.25), and slip on the vertical channels showed moderate increases with each new load level after 200 kips.

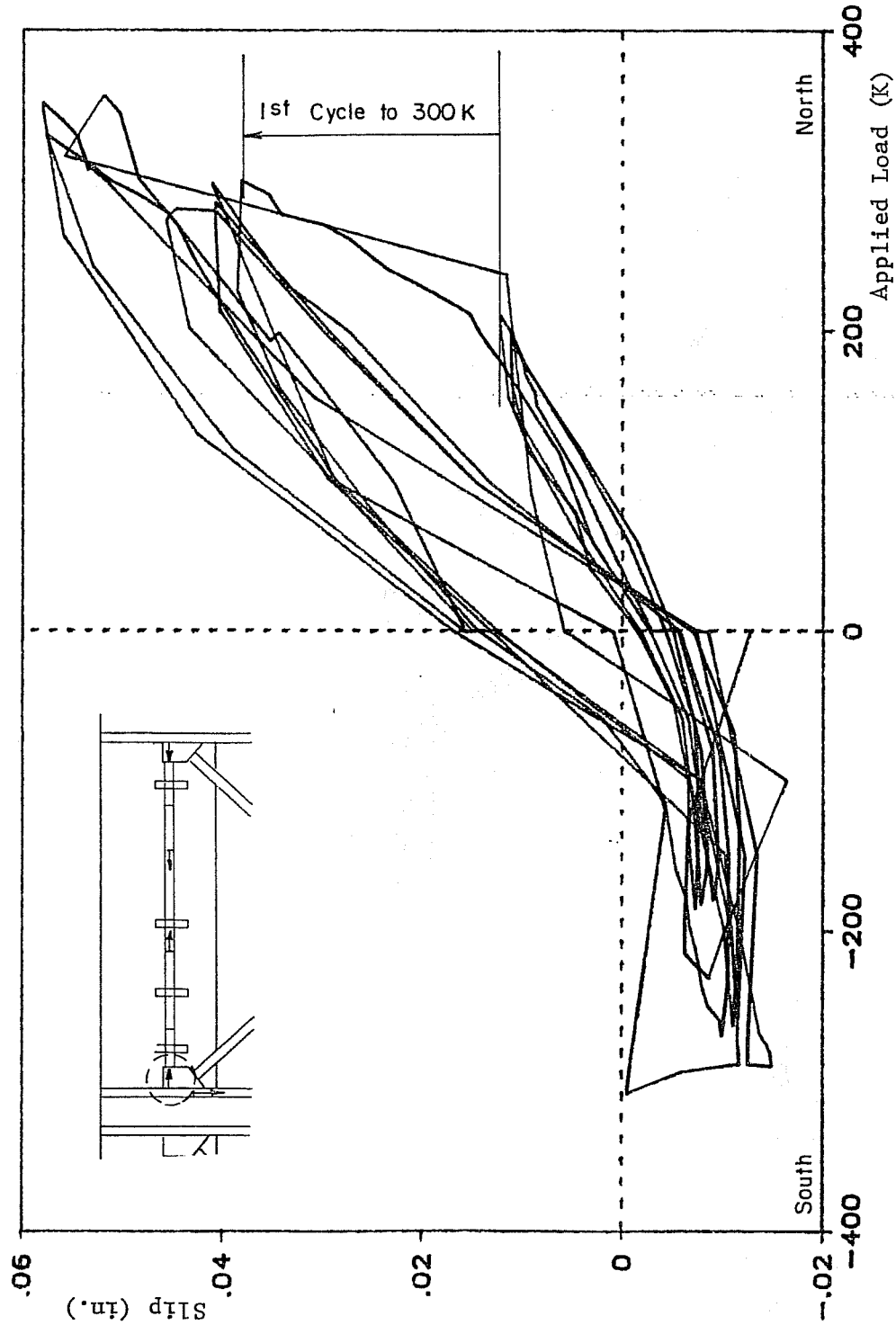


Fig. 5.19 Separation of steel connection from column

The largest displacements were observed at the four locations on the collector at the third level. The two transducers in the middle measured maximum slips of about 0.06 in. when the frame was loaded north and 0.04 in. south. The slips at the ends of the tee were about 0.06 in. north and 0.015 in. when the frame was pushed south. The largest vertical slip observed between the channel and column was .076 in. at the third level. The transducers at the middle connection recorded a maximum displacement of 0.02 in. vertically before they were removed when welds failed.

Figures 5.21 and 5.22 show the load-slip curves for the four instrumented locations on the third level collector for the three cycles to 0.36 percent drift, or about 300 kips lateral load. The curves are similar in shape showing larger slips when the frame was loaded north. The change in slope in the first cycle after 200 kips was attained is apparent.

The same set of load cycles are shown in Fig. 5.23 for the transducers measuring slip between the steel channel and concrete column. For some reason, the slip at the third level was extremely small when the frame was loaded south (channel loaded downward relative to the column).

Figures 5.24 and 5.25 display the strange results obtained from the transducers at the center X-connection. The steel always moved down and to the south relative to the spandrel for loading in both directions. In Fig. 5.25, the increase in slip after 200 kips is shown as well as the increase when the first weld broke. The graph was terminated at this point because there was a large increase in slip each time a weld broke, and the transducers were removed after the third weld failed.

## 5.4 Strains in Concrete Frame

The readings from the strain gages on the spandrel beam longitudinal bars were examined to determine the strains in the concrete frame. The maximum strains in the spandrel bars were about 1000 $in.^{-6}/in.$, approximately half of the strain corresponding to yield of the reinforcing bar.

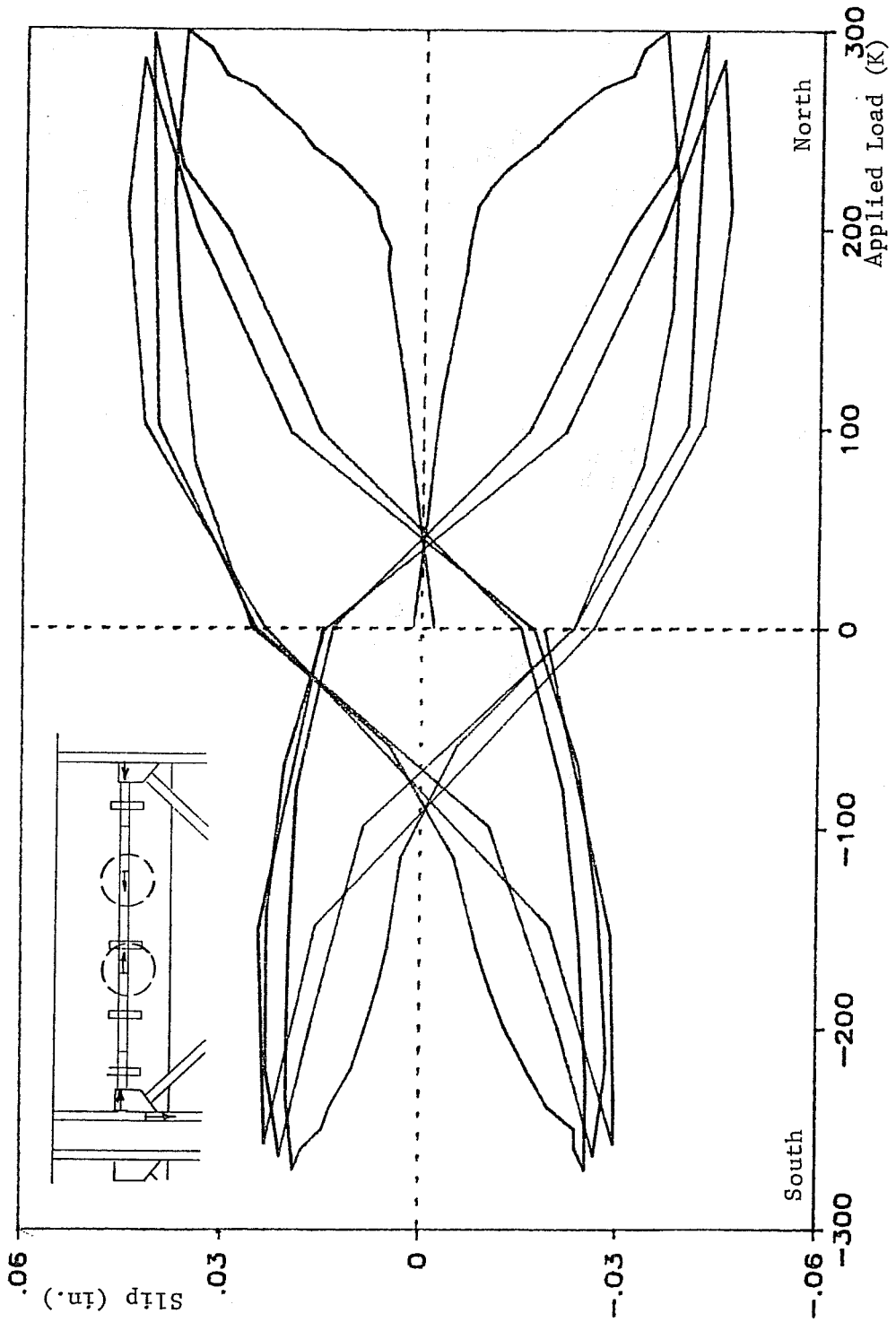


Fig. 5.22 Slips between tee and spandrel - 0.36% drift cycles

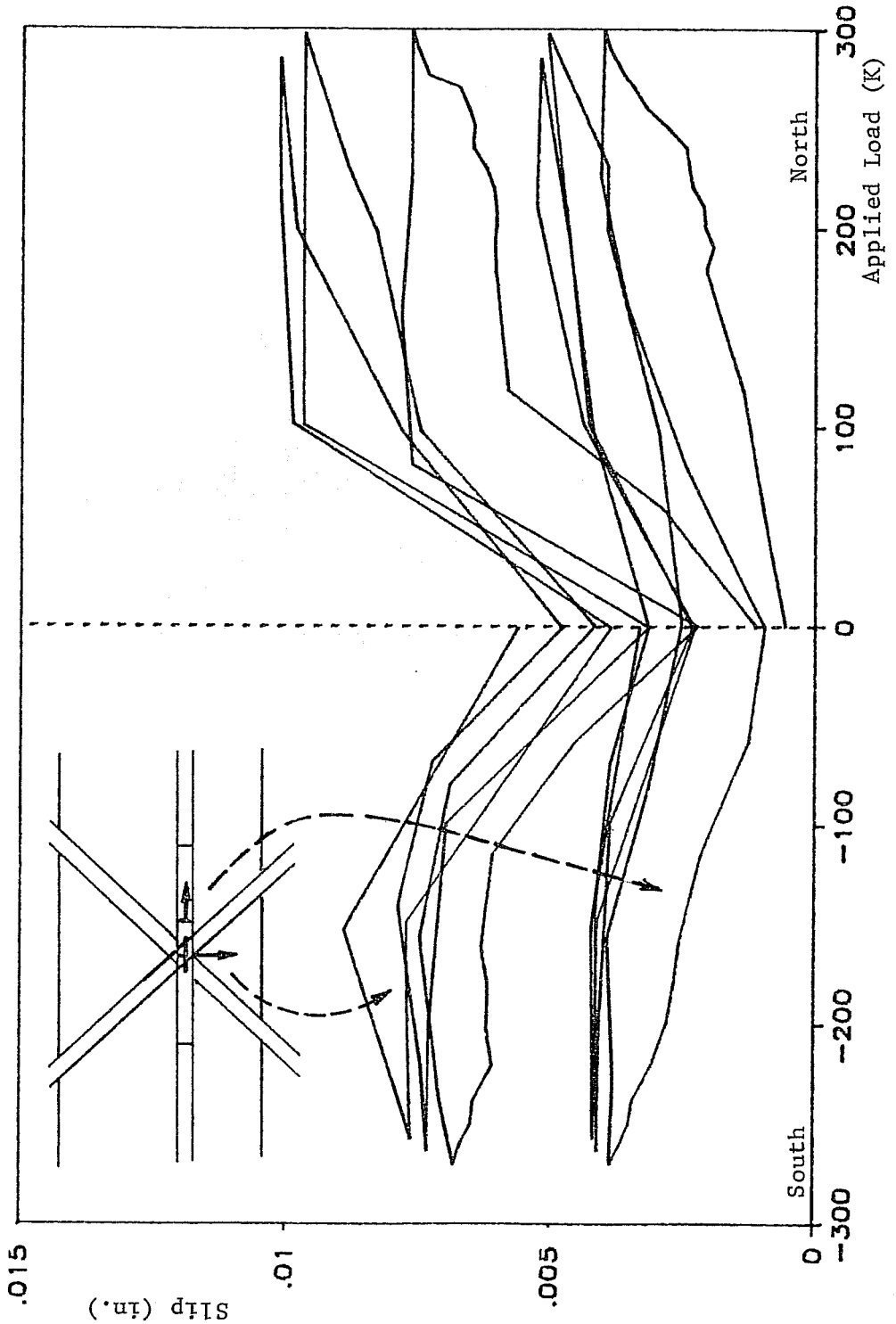


Fig. 5.24 Slips at middle connection - 0.36% drift cycles

# CHAPTER 6

# SUMMARY AND CONCLUSIONS

## 6.1 Summary of Test Program

A two-thirds, scale model of a portion of an exterior frame of a reinforced concrete building was constructed and tested. The two-bay, two-story frame modeled a type of construction popular in California during the 1950's and 1960's which consisted of deep spandrel beams and short, narrow columns. Two strengthening schemes were carried out with the purpose of increasing the lateral load capacity of the model. In this report, the second of these schemes was investigated: erection of a structural steel bracing system.

The exposed diagonal braces were six inch deep wide flange shapes, which were welded at their ends to horizontal and vertical steel collector members. Steel channels were attached to the side faces of the concrete columns with epoxy-grouted threaded rod dowels. The horizontal collectors were structural tees attached in the same manner to the spandrel faces at the floor levels. The braces were designed to carry the entire lateral shear forces computed using the 1982 Uniform Building Code.

The steel braced frame was tested to failure under reversed, cyclic loading. All of the load was applied at the third level of the model near the two columns. Reactions were applied to the frame at corresponding locations in the first level floor slab. Six of the eight braces (all four at the second level and two at the bottom level) were instrumented at mid-length for determination of axial loads.

The model strengthened by steel braces was subjected to seventeen load cycles: two preliminary cycles and five sets of three cycles, with each set at an increased drift level. The maximum loads and drift levels applied to the structure were 360 kips and 1.2 percent drift when the frame was pushed north, and 309 kips and 1.3 percent drift when the frame was loaded south. The peak lateral loads were over three times the computed design earthquake loads. The values represent the interstory drift between the second and third floors of the model, which is where the major damage occurred. Failure at the second level was caused by buckling of the compression braces, local yielding of the tension braces, weld fractures at the ends of the tension

drilled without interference from the steel reinforcement in the columns. In addition, two of the dowels in this region had embedment lengths less than 5-1/2 inches. The need for a sufficient number of dowels with adequate embedment was demonstrated.

An important problem observed in the test of the steel braced frame was the fabrication details of the welded connections; specifically the field welds between the braces and gusset plates. Alternate details and welding procedures were suggested to ensure full penetration of the groove welds. Above all, welding must conform to the requirements specified by the American Welding Society.

The peak loads sustained by the specimen were at least three times the lateral earthquake design loads prescribed by the 1982 UBC. The shear force for the prototype building at the third story (2107 kips for seismic zone 4) divided over sixteen braced bays is 132 kips. For two bays of the two-thirds scale model, the shear force becomes 78 kips. The Uniform Building Code requires braced frames in seismic zones 2,3, and 4 to be designed for 1.25 times the computed lateral earthquake forces. Therefore, the lateral design load for the model frame is 97 kips. At this load level, the braces behaved elastically and continued to perform in a linear manner up to loads of about 290 kips when welds failed and compression braces started to bend.

The design of the steel bracing system did not include the shear strength of the columns in the calculation of the lateral load capacity. However, it was shown that the columns carried between 30 and 40 percent of the applied lateral load. Therefore, it is recommended that the lateral capacity of the system include the nominal shear strength computed from ACI equations (11.2), (11.3.1.1), and (11.17). This would be a conservative estimate of the column capacity because the steel channels approximately doubled the shear strength of the bare column.

## 6.3 Conclusions

The seismic strengthening system consisting of exposed structural steel diagonal braces greatly improved the performance of the reinforced concrete model which had short columns and deep beams making up the exterior frame. The braces carried the lateral loads which would be produced by an earthquake and protected the columns from shear failure. The horizontal and vertical steel collector members transferred the loads and produced good interaction between the concrete frame and steel

## REFERENCES


1. Structural Engineers Association of California, Recommended Lateral Force Requirements and Commentary, Fourth Edition, San Francisco, California, 1975.

2. Wyllie, Loring A., Jr., "Strengthening Existing Concrete and Masonry Buildings for Seismic Resistance," Proceedings of the Second Seminar on Repair and Retrofit of Structures, Ann Arbor, Michigan, 1981, pp. 322-333.

3. Degenkolb, H.J., and Associates, Repair and Strengthening of Reinforced Concrete Structures, San Francisco, California, 1983.

4. Ogura, Koichiro, "Outline of Damages to Reinforced Concrete Structures," Proceedings of U.S.-Japan Seminar on Earthquake Engineering with Emphasis on the Safety of School Buildings, Sendai, Japan, 1970.

5. Higashi, Y., "Strengthening of Reinforced Concrete Structures," Research Report, Higashi Laboratory, Tokyo, Japan, 1981.

6. Sugano, S., "An Overview of the State-of-the-Art in Seismic Strengthening of Existing Reinforced Concrete Buildings in Japan", Proceedings of the Third Seminar on Repair and Retrofit of Structures, Ann Arbor, Michigan, 1982, pp. 328-349.

7. Sugano, S., "Guideline for Seismic Retrofitting (Strengthening, Toughening and/or Stiffening) Design of Existing Reinforced Concrete Buildings," Proceedings of the Second Seminar on Repair and Retrofit of Structures, Ann Arbor, Michigan, 1981, pp. 189-237.

8. Shimizu, Y., Higashi, Y., Endo, T., and Ohkubo, M., "Aseismic Capabilities of Strengthened Reinforced Concrete Frame," Research Report, Higashi Laboratory, Tokyo, Japan, 1981.

9. Sugano, S., and Endo, T., "Seismic Strengthening of Reinforced Concrete Buildings in Japan," Strengthening of Building Structures - Diagnosis and Theory, IABSE Symposium, Venice, Italy, 1983, pp. 371-378.

10. Kawamata, S., and Ohnuma, M., "Strengthening Effect of Eccentric Steel Braces to Existing Reinforced Concrete Frames," Proceedings of the Second Seminar on Repair and Retrofit of Structures, Ann Arbor, Michigan, 1981, pp. 262-269.

24. Roach, C. E., and Jirsa, J. O., "Seismic Strengthening of a Reinforced Concrete Frame Using Reinforced Concrete Piers," PMFSEL Report NO. 86-4, The University of Texas at Austin, May 1986.